DRAFT

CAL/APT PROGRAM: TEST RESULTS FROM ACCELERATED PAVEMENT TEST ON PAVEMENT STRUCTURE CONTAINING ASPHALT TREATED PERMEABLE BASE (ATPB)—SECTION 502CT

Report Prepared for

CALIFORNIA DEPARTMENT OF TRANSPORTATION

by

J. Harvey, I. Guada, C. Scheffy, L. Louw, J. Prozzi, D. Hung

November 1998
Pavement Research Center
Institute of Transportation Studies
University of California, Berkeley

DISCLAIMER

FINANCIAL DISCLOSURE STATEMENT

This research has been funded by the Division of New Technology and Research of the State of California Department of Transportation (contract No. RTA-65W485). The total contract amount for the initial five year period (1 July 1994 through 30 June 1999) was $5,751,159[1]. This report presents the results of the third HVS test completed in September 1996 on a pavement section containing asphalt treated permeable base. The report provides an analysis of the test results and conclusions which contain implications for Caltrans pavement design and pavement construction practices.

IMPLEMENTATION STATEMENT

Results of this HVS test, like that on the previously tested sections—500RF, 501RF, and 503RF, demonstrate the importance of mix compaction on pavement performance (both fatigue and permanent deformation) and show that the improved pavement performance which results from improved compaction can result in large, quantifiable savings to the State.

---

[1] Prior to the completion of this report the contract was amended to extend the completion date to 30 June 2000 and the contract total was increased to $12, 804, 824.

As in the previous sections, a weak bond was observed between the asphalt-concrete lifts in the sections which was found to significantly degrade pavement performance. The recommendations contained in the earlier reports relative to the use of a tack coat are confirmed by the results of this test as well.

ACKNOWLEDGMENTS

Financial support for this project was provided by the State of California Department of Transportation as part of the CAL/APT Project. Mr. Wesley Lum of the Division of New Technology and Research is the CAL/APT Project Manager and Mr. William Nokes, Office of Project Planning and Design, served as the Contract Monitor during the period of the test for the University of California, Berkeley contact.

TABLE OF CONTENTS

LIST OF FIGURES

LIST OF TABLES

EXECUTIVE SUMMARY

This report is the third in a series which describe the results of tests and their interpretation on full-scale pavements designed and constructed according to the procedures of the California Department of Transportation (Caltrans) at the Richmond Field Station (RFS) of the University of California at Berkeley (UCB). It describes the results of the Heavy Vehicle Simulator (HVS) test on the *third* of *four* pavement test sections, an asphalt-concrete section containing an asphalt treated permeable base (ATPB) designated Section 502CT. The tests on these four test sections have been performed as part of Goal 1 of the Strategic Plan of the Caltrans Accelerated Pavement Testing, or CAL/APT program *(1)*.

One objective of the test program is to obtain data to quantitatively verify existing Caltrans pavement design methodologies for asphalt treated permeable base (ATPB) pavements and conventional aggregate base pavements with regard to failure under trafficking at moderate temperatures (Goal 1), while preparing a uniform platform on which overlays (Goal 3) will be constructed to be trafficked. Other objectives are:

- to quantify the effective elastic moduli of the various pavement layers, based on an ad-hoc use of layered elastic analysis;
- to quantify the stress dependence of the pavement layers;
- to determine the failure mechanisms of the various layers; and
- to determine and compare the fatigue lives of the two types of pavement structure.

HVS loading on this pavement section began in December 1995 and was completed in September 1996 after the application of about 2.67×10^6 load repetitions. At the end of the

test, cracking had reached a level which, according to Caltrans pavement management criteria, resembled a newer pavement that had failed by alligator cracking.

Chapter 2 describes the test program for Section 502CT. Design thicknesses for the pavement components for a Traffic Index of 9.0 (1.0 million ESALs) were: aggregate subbase—229 mm (0.75 ft); aggregate base—182 mm (0.60 ft); asphalt treated permeable base—76 mm (0.25 ft); and asphalt concrete—137 mm (0.45 ft). Actual thicknesses at the loading site were: aggregate subbase—215 mm (1.00 ft); aggregate base—182 mm (0.60 ft); asphalt treated permeable base—76 mm (0.25 ft); and asphalt concrete—148 mm (0.48 ft).

Table 2.1 summarizes the data collection program for Section 503CT. Loading, applied by dual bias-ply tires inflated to a pressure of 690 kPa (100 psi), consisted of 150,000 repetitions of a 40 kN (9,000 lb) load followed by 50,000 repetitions of a 80 kN (18,000 lb) and then by about 2.47 million repetitions of a 100 kN (22,500 lb) load. At the termination of loading, fatigue cracking was visible throughout the test section. Lateral wander of the wheels over the one meter (3.3 ft) width of the section was the same as for the other three test sections (500RF, 501RF, 503RF).

Chapter 3 summarizes the data obtained during the course of loading. Pavement response measurements were obtained using Multi-Depth Deflectometers (MDDs), the Road Surface Deflectometer (RSD), the laser profilometer, and a straight edge. Fatigue crack development was monitored using photographs and analyzed using a digital image analysis procedure. Thermocouples were used to measure the air temperature and pavement temperatures at various depths in the asphalt concrete. To maintain a reasonably consistent temperature of about 20°C, a temperature control cabinet (“cold box”) was installed.

As with the other three sections, cracking appears to have occurred in only the top lift of the aggregate concrete layer. Moreover, it was observed, from a limited coring program after the HVS testing was completed, that there appeared to be little or no bond between the two lifts used to achieve the constructed thickness of the aggregate concrete layer and no bonding occurred under the HVS trafficking at 20°C. In addition, measurements indicate that the lower asphalt concrete lift was compacted to an average air-voids content of 4.0 percent and the upper lift had similar compaction, i.e. to an average air-voids content of about 7.6 percent.

The 2.67 million repetitions applied to Test Section 501RF corresponds to about 117 million ESALs (based on the Caltrans load equivalency factor of 4.2). Chapter 4 provides a detailed analysis of the test results using multilayered elastic analysis to explain the observed behavior.

Results of the analysis reported in Chapter 4 indicate a reasonable correspondence between the Caltrans design estimate of approximately 1,000,000 ESALs and the HVS test measurement of approximately 117,000,000 ESALs. An impediment to reconciling these two estimates has been the inability to accurately quantify effects of the layer interface condition. The following findings of this aspect of the study are considered to have been reasonably well demonstrated and to represent appropriate hypotheses for future inquiry and validation:

1. Fatigue life measurements under full-scale accelerated loading are typically expected to exceed design estimates because design estimates must incorporate a safety factor to minimize the risk of premature failure while accommodating, at the same time, expected variability in testing, in construction, in traffic, and in mix design. As it was shown for Test Section 500RF, which has the same structural design as Test Section 502CT, for a design reliability level of 90

percent, the computed ratio of simulated HVS ESALs to design ESALs estimated using the fatigue analysis and design system was approximately 3.7.

2. The mix fatigue analysis and design system proved to be an effective tool for explaining fatigue performance of the HVS pavement. The relatively good agreement between the simulation estimate and actual HVS measurement reinforces earlier recommendations that the analysis and design system should prove useful for structural design as well as for mix design.

3. According to Asphalt Institute's subgrade strain criteria, severe rutting associated with permanent deformations in the unbound layers in the HVS pavement would not be expected. Testing of HVS Section 502CT generally confirmed this.

4. The analyses reported herein corroborate prior work showing the importance of good compaction of the asphalt concrete surface to superior fatigue performance. Good compaction of the mix also reduces the amount of rutting contributed by the unbound pavement layers.

5. Loss of bond at the interface between asphalt-concrete lifts can cause a significant reduction in fatigue life and an increase in rutting resulting from increased stresses in the unbound layers.

6. Different mixes, even with similar binders, can result in significantly different fatigue performance. The importance and effectiveness of laboratory fatigue testing and simulation to quantitatively estimate differences in fatigue performance in situ were demonstrated by analyses presented this chapter.

Chapter 5 contains the conclusions which are as follows:

1. The fatigue analysis and design system developed during the SHRP program and refined within the CAL/APT program has been used to explain the difference between the design estimate for Section 502CT of approximately one million ESALs and the HVS measurement of approximately 117 million ESALs. Although some of the discrepancy remains unaccounted for (possibly as a result of difficulties in modeling the bonding between the two lifts of asphalt concrete), the overall agreement helps to validate both the analysis and design system as a mechanism for structural design and provides some indication of the limits of validity of the current Caltrans design methodology.

2. As with Sections 500RF and 501RF, results of this HVS test suggest that the Asphalt Institute's subgrade strain criteria to control rutting resulting from permanent deformations in the unbound layers is a reasonable design parameter. Accordingly, these criteria are suitable for use in mechanistic/empirical analyses of rutting to supplement routine Caltrans design procedures in special investigations.

3. Results of the 502CT test support those from 500RF and suggest that the Caltrans structural design procedure for a Traffic Index of 9 provides a design reliability of about 90 percent for pavements with ATPB, typical compaction and representative asphalt concrete mixes. This result is based on the assumption that the stiffness of the asphalt treated permeable base is not reduced by water action. Results of laboratory repeated-load tests, also completed as a part of Goal 1, indicate that stripping of the asphalt treated permeable base may lead to an unconservative design. The analysis and design system used herein and being refined through the CAL/APT program can provide an improved methodology for structural pavement design

permitting a higher level of reliability in the design process. This type of approach should be beneficial to the design of long-life asphalt pavements, an emerging concern to Caltrans.

4. The recommendations regarding mix compaction and tack coat application resulting from the Sections 500RF and 501RF tests are supported by the results obtained from Section 502CT.

CHAPTER 1

INTRODUCTION

This report is the third in a series which describe the results of accelerated pavement tests with the Heavy Vehicle Simulator (HVS) on full-scale pavements designed and constructed according to the procedures of the California Department of Transportation (Caltrans) at the Richmond Field Station (RFS) of the University of California at Berkeley (UCB). It contains a summary of the results of HVS tests and their interpretation on the fourth pavement test section; an asphalt-concrete section containing an asphalt treated permeable base designated Section 502CT. Tests on the four test sections have been performed as part of Goal 1 of the Strategic Plan of the Caltrans Accelerated Pavement Testing, or CAL/APT Program *(1)*.

The first report covering this phase of the program, entitled *Initial CAL/APT Program: Site Information, Test Pavements Construction, Pavement Materials Characterizations, Initial CAL/HVS Test Results, and Performance Estimates* contains detailed information on the construction of the test pavements, as well as results of tests that define the properties of the various pavement components of the four pavement test sections *(2)*. Completed reports describing the HVS tests in the individual sections include:

- *CAL/APT Program: Test Results from Accelerated Pavement Test on Pavement Structure Containing Asphalt-Treated Permeable Base (ATPB)—Section 500RF* contains detailed information on the HVS test of the other ATPB, Section 500RF *(3)*[2],

[2] A separate report describing the performance of ATPB under saturated conditions in laboratory repeated load tests; performance estimates of pavements containing saturated ATPB through simulation; and a review of Caltrans experience ATPB has also been prepared *(4)*. A report has also been prepared presenting analyses and comparisons

- *CAL/APT Program: Test Results from Accelerated Pavement Test on Pavement Structure Containing Aggregate Base—Section 501RF* contains detailed information on the HVS test of the aggregate base Section 501RF *(6)*,
- *CAL/APT Program: Test Results from Accelerated Pavement Test on Pavement Structure Containing Aggregate Base—Section 503RF* contains detailed information on the HVS test of the aggregate base Section 503RF *(7)*.

The information and findings presented in this report support the recommendations regarding changes in Caltrans construction and construction control procedures presented in the earlier reports, e.g. Reference *(3)*.

1.1 OBJECTIVES

The main objective of this test plan, described in Reference *(2)*, is to develop data to quantitatively verify existing design methodologies for asphalt treated permeable base (ATPB) pavements and conventional aggregate base pavements with regard to failure under trafficking at moderate temperatures. Other objectives include:

- quantification of the effective elastic moduli of the various pavement layers, based on an ad-hoc use of layered elastic analysis;
- quantification of the stress dependence of the pavement layers;
- definition of the failure mechanisms of the various layers; and
- determination and comparison of the fatigue lives of the two types of pavement structures (drained versus undrained).

---

of the Caltrans and AASHTO flexible pavement design methods *(5)*.

1.2 PURPOSE AND SCOPE

This report presents the results of tests and associated analyses for Section 502CT. The scheduled sequence of HVS testing of the four test sections has been: 1) drained ATPB site, 500RF; 2) undrained aggregate base site, 501RF; 3) drained ATPB site, 502CT; and 4) undrained aggregate base site, 503RF.

1.3 ORGANIZATION OF REPORT

Chapter 2 of the report contains a complete description of the test program performed on Section 502CT, including the loading sequence, instrumentation, and data collection scheme. Chapter 3 presents a summary and discussion of the data collected during the test, including pavement performance and temperatures. In Chapter 4, the actual pavement performance is compared with the fatigue life predicted for the test section using the Caltrans thickness design procedure. Analyses are presented which evaluate the effects of construction variables, mix characteristics and temperature environment on the fatigue life and permit extrapolation of the HVS test results to Caltrans' in-service pavements. The HVS results are shown to validate the analyses. Chapter 5 contains a summary of the results and conclusions drawn from them.

CHAPTER 2

TEST PROGRAM

2.1 TEST SECTION LAYOUT

The test section layout is described in detail in Reference *(3)*. Test site 502CT is one of the drained sections; that is, it includes a layer of asphalt treated permeable base (ATPB) resting on aggregate base. Locations of the four test sections are indicated in Figure 2.1.

The pavement structure (Figure 2.2) was designed according to Caltrans procedures *(8)* and consists of a clay subgrade (AASHTO A-7-6), aggregate subbase, aggregate base, asphalt treated permeable base (ATPB), and asphalt concrete. Construction control data for this section are contained in Reference *(2)*.

Design thicknesses of the pavement components are: aggregate subbase, 229 mm; aggregate base, 182 mm; ATPB, 76 mm; and asphalt concrete, 137 mm. The aggregate subbase thickness varies across the section reflecting the 2 percent cross fall of the pavement *(2)*. Measurements from cores and elevations taken on each compacted layer indicate the following constructed thicknesses: asphalt concrete upper lift, 68 mm; asphalt concrete lower lift, 80 mm; ATPB, 76 mm; aggregate base, 182 mm; aggregate subbase, 215 mm (average).

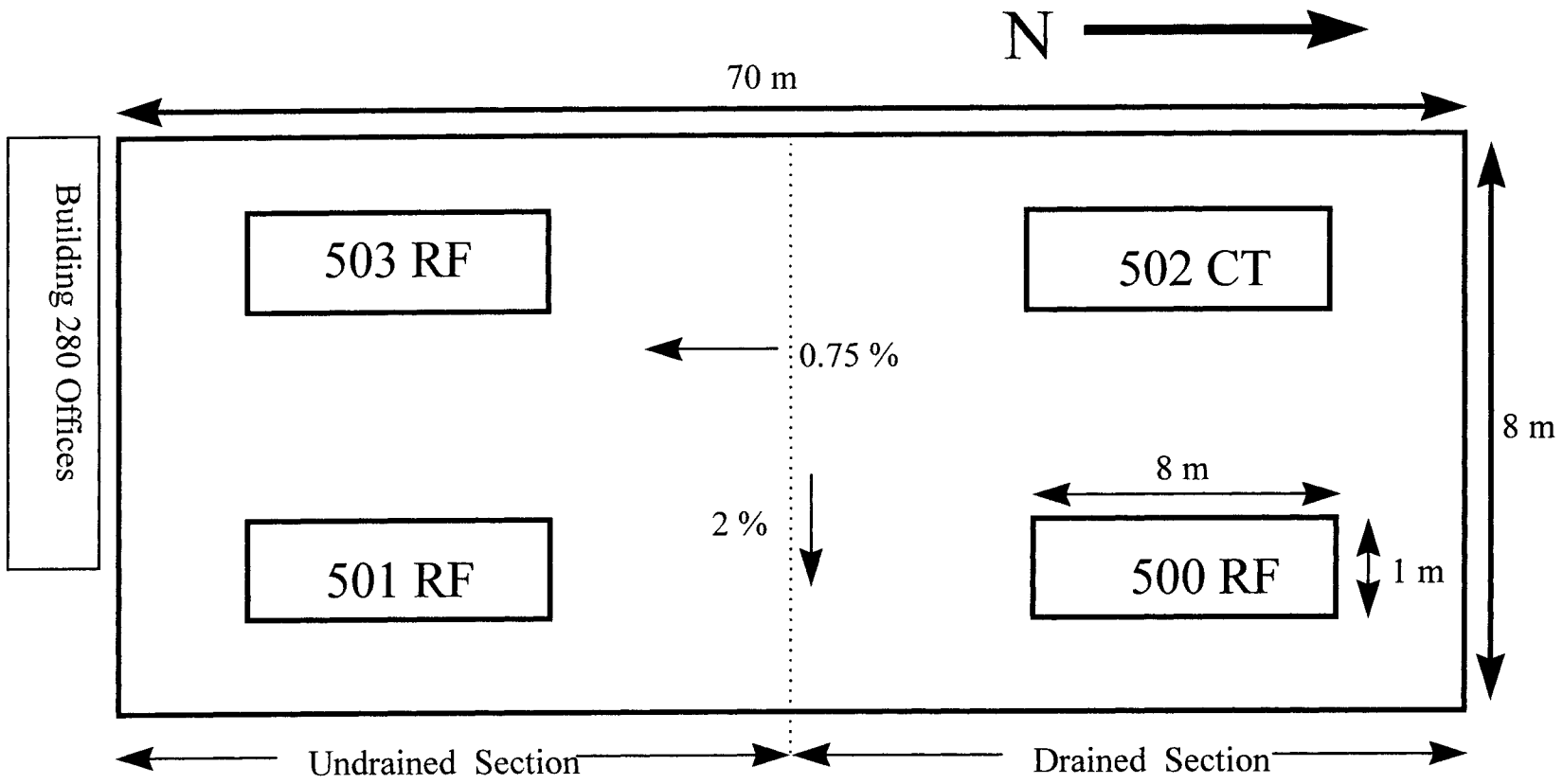

Figure 2.1 Layout of Goal 1 sections

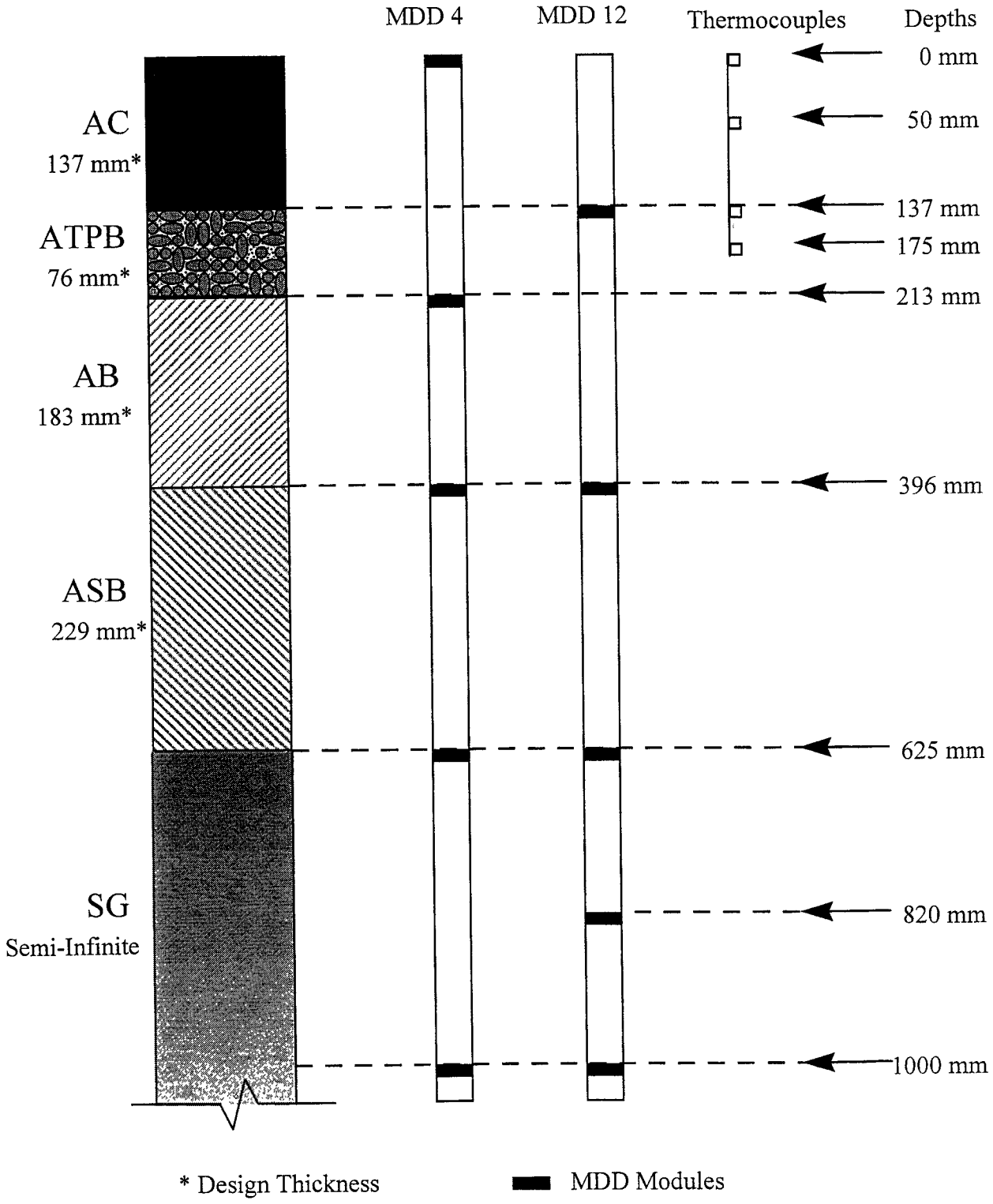

Figure 2.2 502CT pavement structure with MDD and thermocouple positioning

2.2 TEST PROGRAM

2.2.1 Loading Program

HVS loading on this pavement section was initiated in December 1995 and completed in September 1996 after the application of more than 2.67×10^6 load repetitions. At this point, cracking had reached a level which, according to Caltrans pavement management criteria, resembled a pavement that had failed by alligator cracking.

The HVS test program followed for Section 502CT is summarized in Table 2.1. This table shows the data collection schedule during the course of the test. The loading applied to Section 502CT is similar to that applied to Section 500RF as described in Reference *(3)*. It should be noted that HVS 2 was used for this section whereas HVS 1 was used for tests on 500 RF, 501 RF and 503 RF. As shown in Table 2.1, a load of 40 kN was used to traffic the section for the first 150,000 repetitions in order to prevent excessive damage to the newly constructed asphalt concrete pavement. After 150,000 repetitions at 40 kN, the load was increased to 80 kN for 50,000 repetitions. Then, at 200,000 repetitions, the load was increased to 100 kN; this load was maintained for the remainder of the test to accelerate pavement damage.

The HVS was equipped with dual bias-ply truck tires inflated to a pressure of 690 kPa. Lateral wander over the 1 meter width of the test section is programmed to simulate traffic wander on a typical highway lane (3.7 m wide)[3].

---

[3] Reference *(3)* summarizes the lateral load distribution (wander) used in this test.

Table 2.1 Data collection program for test Section 502CT

Repetitions	Trafficking Load kN	Rut Profiles	MDD				RSD											
							Centerline				200 mm Left*				200 mm Right*			
			Test Wheel Load, kN				Test Wheel Load, kN				Test Wheel Load, kN				Test Wheel Load, kN			
			40	60	80	100	40	60	80	100	40	60	80	100	40	60	80	100
10	40	X	X				X				X				X			
15,000-45,000 (15,000 incr)	40	X	X				X				X				X			
70,000	40	X	X				X				X				X			
100,000	40	X	X				X				X				X			
125,000	40	X	X				X				X				X			
150,000	40 to 80	X	X	X	X		X	X	X		X	X	X		X	X	X	
175,000	80	X	X		X		X		X		X		X		X		X	
200,000	80 to 100	X	X	X	X	X	X	X	X	X	X	X	X	X	X	X	X	X
225,000	100	X	X			X	X			X								
250,000	100	X	X			X	X			X								
300,000	100	X	X			X	X			X								
350,000	100	X	X			X	X			X								
400,000 to final (400,000 incr)	100	X	X		X	X	X		X	X	X		X	X	X		X	X
450,000 to final (50,000 incr)	100	X	X			X	X			X	X			X	X			X
Crack Appearance (1,298,222)	100	X	X		X	X	X		X	X	X		X	X	X		X	X
Final (2.673,589)	100	X	X	X	X	X	X	X	X	X	X	X	X	X	X	X	X	X

*Looking in direction of increasing longitudinal reference points (0-16)

2.2.2 Measurements

To evaluate pavement response during HVS testing of Section 502CT, measurements were obtained using the following:

- Multi-Depth Deflectometer (MDD);
- Road Surface Deflectometer (RSD);
- Laser Profilometer; and
- straight edge.

Surface crack development was monitored using photographs and digital image analysis techniques. Thermocouples were used to measure the air temperature and pavement temperatures at various depths in the asphalt concrete. Detailed descriptions of the instrumentation and the various measuring equipment are included in References *(2)*, *(3)*, and *(9)*.

RSD surface deflection data were obtained at the reference points along the section centerline and at locations 200 mm on each side of the centerline, Figure 2.3. These latter measurements, taken off the centerline where the wander pattern results in fewer load applications, assist in characterizing the full test section. Measurements of transverse surface rut depth using the laser profilometer permit determination of:

- the location and magnitude of the maximum rut;
- the average rut throughout the test section; and
- the rate of permanent deformation, or development (rutting rate).

Permanent deformations occurring in the layers during the test are measured using the MDDs at the two locations shown in Figure 2.3, Points 4 and 12. The surface deflection

measured at the MDD at Point 4 provides a check on the RSD deflection measured at this point.

All pavement temperature measurements using the thermocouples (locations shown in Figures 2.2 and 2.3) were obtained at one-hour intervals during HVS operation. Air temperatures near the test section were recorded at the same intervals and at the time of data collection.

Visual observation of surface distress was primarily directed to the identification and demarcation of surface cracks as well as measurements of their lengths. It should be noted that at the conclusion of testing of the overlaid Section 502CT, a trench will be dug to allow visual inspection and measurement of all the layers and to obtain material for laboratory testing. This trench and visual inspection of the pavement layers will provide essential data and clarify any inconsistencies generated during the test.

Depths at which the multi-depth deflectometers (MDDs) and thermocouples were placed are shown in Figure 2.2, while their locations on the surface of the test section are shown in Figure 2.3. Positions at which deflections were measured with the road surface deflectometer are also shown in Figure 2.3. Intervals between measurements (Table 2.1), in terms of load repetitions, were selected to insure adequate characterization of the pavement as damage accumulated.

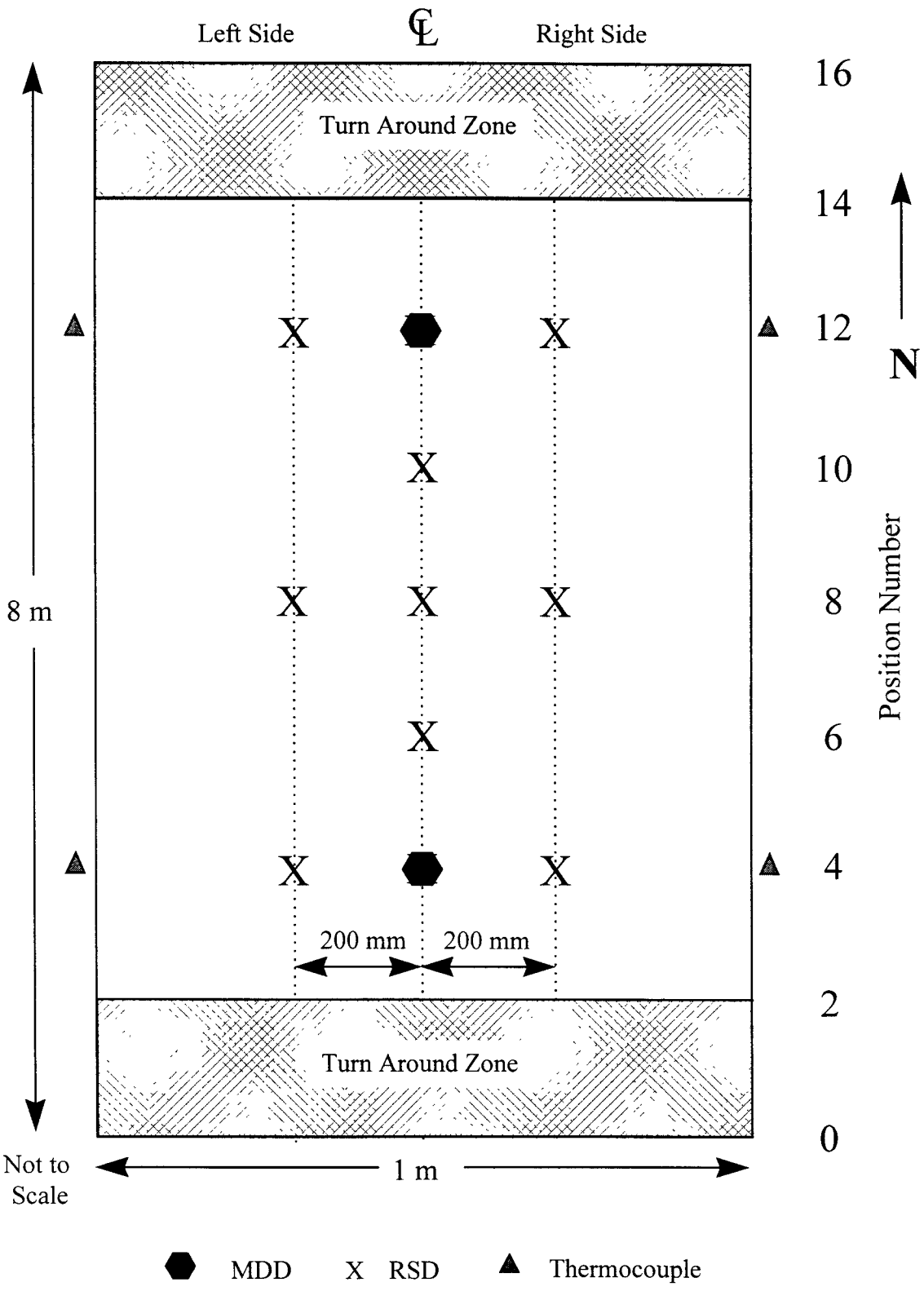

Figure 2.3 Plan view of test section and location of instruments for data collection

2.3 ENVIRONMENTAL CONDITIONS

Temperature has an important influence on the fatigue performance of a pavement. To maintain a fairly constant temperature, a temperature control cabinet, or "cold box," was installed on the HVS test carriage. It was desired that the pavement surface temperature remain at approximately 20°C throughout the test to reduce the potential for rutting of the asphalt concrete surface, and to provide a relatively uniform test temperature similar to that in the other sections. The temperature range during the test was larger than for the 501RF and 503RF tests.[4]

Since the test pavements are located in the indoor facility, the pavement surfaces receive no direct rainfall. However, the test sections are subject to water infiltration since they have been constructed on the natural subgrade. Water can access the pavement from outside the building due to horizontal movement as well as from the ground water table. As noted in Reference *(2)*, a drainage system was installed around the outside of the building to reduce the potential for this horizontal flow. It must be emphasized that this external drainage system is separate from the ATPB layer and edge drain constructed in the test pavement.

[4] The cold box constructed for HVS2 was not as effective in maintaining a uniform temperature as that used with HVS1.

CHAPTER 3

DATA SUMMARY: TEMPERATURES, PERMANENT DEFORMATIONS, ELASTIC DEFLECTIONS, CRACKING

This chapter provides a summary of the data obtained as well as a brief discussion of the results. Interpretation of the data in terms of pavement performance is discussed in Chapter 4.

3.1 TEMPERATURES

Pavement temperatures for the entire testing period of Section 502CT ranged from 10°C to 25°C. As reported in Reference *(3)*, temperatures for Section 500RF ranged between 13°C to 36°C. While the temperature range for Section 502CT was less than that for Section 500RF, it was wider than that for Sections 501RF and 503RF.

In addition to air temperatures, pavement temperatures were monitored and recorded regularly for the duration of the entire test, as was done during tests on the other three sections.

3.1.1 Air Temperature in the Temperature Control Unit

Air temperatures measured within the cold box are presented in Figure 3.1. Daily averages, which varied from 10°C to 25°C, were calculated from the hourly temperatures taken during HVS operation. As noted in Figure 3.1, the average air temperatures exhibited a slightly cooling trend in December. These temperatures then increased from January until the

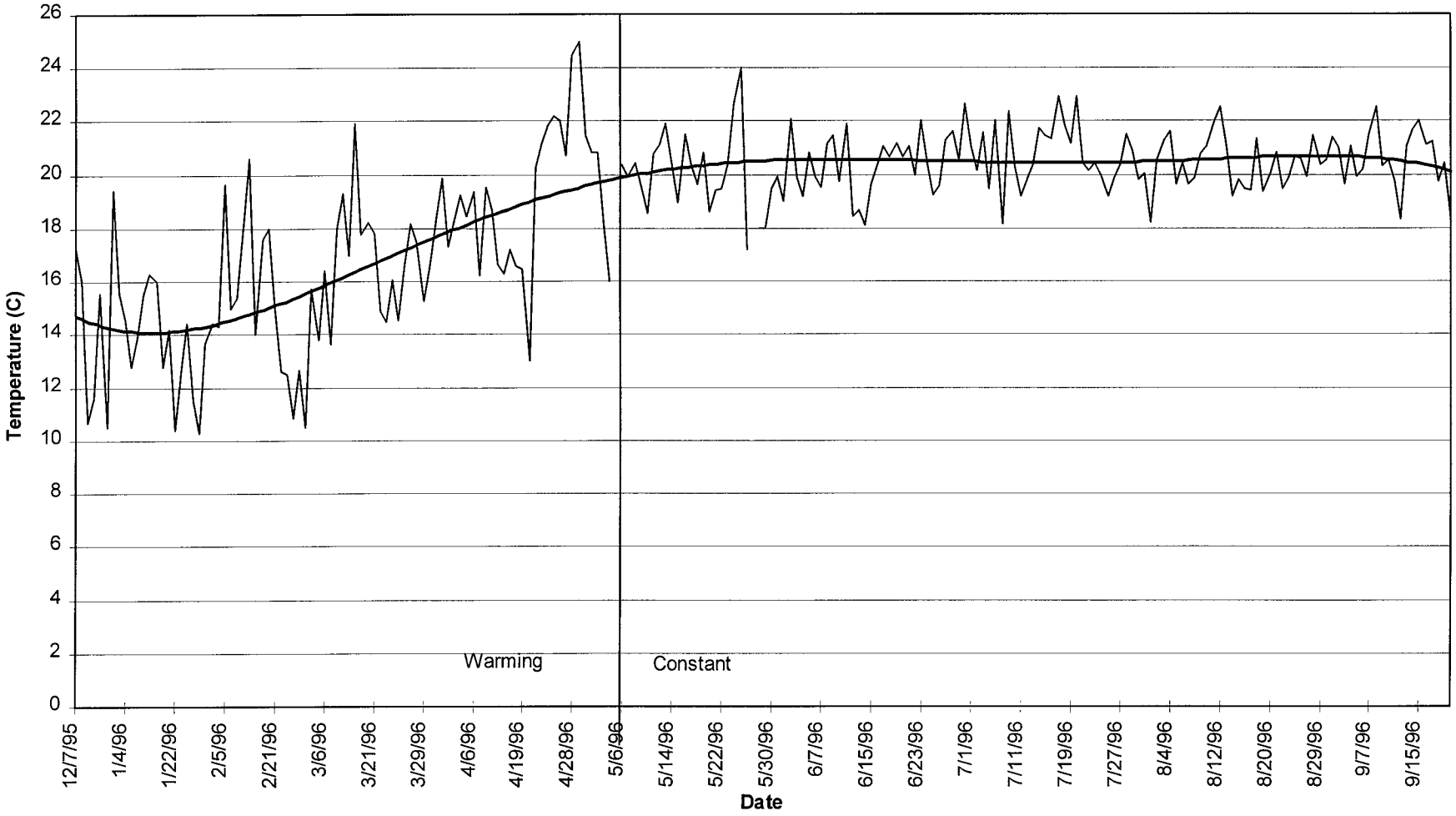

Figure 3.1 Daily average air temperature for the entire testing period of Section 502CT

end of April, reflecting the local conditions. From May until the end of the test, air temperatures remained fairly constant near 20°C as seen in Figure 3.1. Air temperatures during December, January, and February were slightly below the range (20°C ± 4°C) which had been at for the test program.

Average air temperatures for 6-hour periods during the day are shown in Table 3.1. These temperatures represent the average for all of the temperatures measured in each period during the course of the test. As seen in the table, highest air temperatures occurred during the 1300 to 1800 period with an average of 21.5°C.

Table 3.1 Average temperature (°C) over 6-hour intervals for air, surface, and in-depth levels

TIME PERIOD	Air Temp (°C)		Surface Temp (°C)		In-depth temperatures (°C)					
					50 mm		137 mm		175 mm	
	Avg	Std	Avg	Std	Avg	Std	Avg	Std	Avg	Std
0100-0600	18.1	2.2	20.5	1.9	21.1	1.7	20.8	1.4	21.4	1.6
0700-1200	18.1	3.8	19.6	2.8	19.6	2.8	19.9	2.2	19.7	2.9
1300-1800	21.5	3.6	21.4	2.4	21.2	2.3	21.1	1.8	20.9	2.4
1900-2400	19.8	2.5	21.5	1.7	21.8	1.5	21.5	1.3	21.9	1.4
Maximum* Difference	3.4		1.9		2.2		1.6		2.2	

* difference between minimum and maximum 6-hour interval averages

The average air and surface temperature data are compared with the corresponding data from Sections 500RF, 501RF, and 503RF in Table 3.2a, while similar data in the average in-depth temperatures are shown in Table 3.2b. It will be noted that the average temperatures in 502CT are slightly higher than those for 501RF and 503RF and less than those for 500RF.

Table 3.2 Average temperature data over 6-hour intervals for the four test sections

a. Air and surface temperatures

Time Period	Air Temperature °C								Surface Temperature °C							
	500RF		501RF*		502CT		503RF		500RF		501RF		502CT		503RF	
	Avg.	St. Dev.	Avg.	St. Dev.	Avg.	St. Dev.	Avg.	St. Dev.	Avg.	St. Dev.	Avg.	St. Dev.	Avg.	St. Dev.	Avg.	St. Dev.
0100-0600	19.3	—	15.0	2.3	18.1	2.2	19.9	2.3	23.8	—	18.6	1.3	20.5	1.9	20.2	1.7
0700-1200	21.3	—	16.5	2.5	18.1	3.8	20.0	2.5	23.4	—	18.1	1.6	19.6	2.8	20.1	1.6
1300-1800	25.1	—	18.1	2.5	21.5	3.6	20.9	2.7	25.3	—	19.6	1.3	21.4	2.4	20.3	1.7
1900-2400	21.3	—	16.2	2.3	19.8	2.5	20.5	2.4	24.7	—	19.2	1.2	21.5	1.7	20.4	1.6
Max. difference	5.8		3.1		3.4		1.0		1.9				1.9		0.4	

* Outside of temperature control box.

b. In-depth temperatures

Time Period	Depth: 50 mm				Depth: 137 mm				Depth: 175 mm			
	500RF	501RF	502CT	503RF	500RF	501RF	502CT	503RF	500RF	501RF	502CT	503RF
0100-0600	24.2	18.8	21.1	20.5	24.6	19.0	20.8	20.7	24.6	19.1	21.4	20.8
0700-1200	23.5	17.9	19.6	20.2	23.8	18.1	19.9	20.4	24.0	18.1	19.7	20.5
1300-1800	25.2	19.6	21.2	20.4	24.7	19.4	21.1	20.5	24.7	19.6	20.9	20.5
1900-2400	24.9	19.4	21.8	20.6	25.0	19.5	21.5	20.7	24.9	19.5	21.9	20.8
Max. Difference	1.7	1.7	2.2	0.4	1.2	1.4	1.6	0.3	0.9	1.5	2.2	0.3

3.1.2 Surface Temperature

Daily averages of the pavement temperature at different depths are shown in Figure 3.2. These temperatures have a less pronounced warming and cooling trend than the daily average ambient temperatures, and surface temperatures were generally greater on average than were air temperatures.

Table 3.3 presents the average temperatures for two distinct temperature periods during the test, labeled the warming trend and the constant trend (See Figure 3.1). The figure shows that regardless of the trend in temperature, the average temperature at the surface of the pavement is greater than the average air temperature.

Table 3.3 Average daily temperature

Trends, Dates, and Repetitions	**Warming 12/5/95–5/5/96 10–839,258**	**Constant 5/6/96–9/20/96 839,259–2,673,589**
Level	**Average Temperature (° C)**	
Air	17.2	20.4
Surface	19.5	21.4
50 mm	19.4	21.7
137 mm	19.6	21.2
175 mm	19.1	21.8

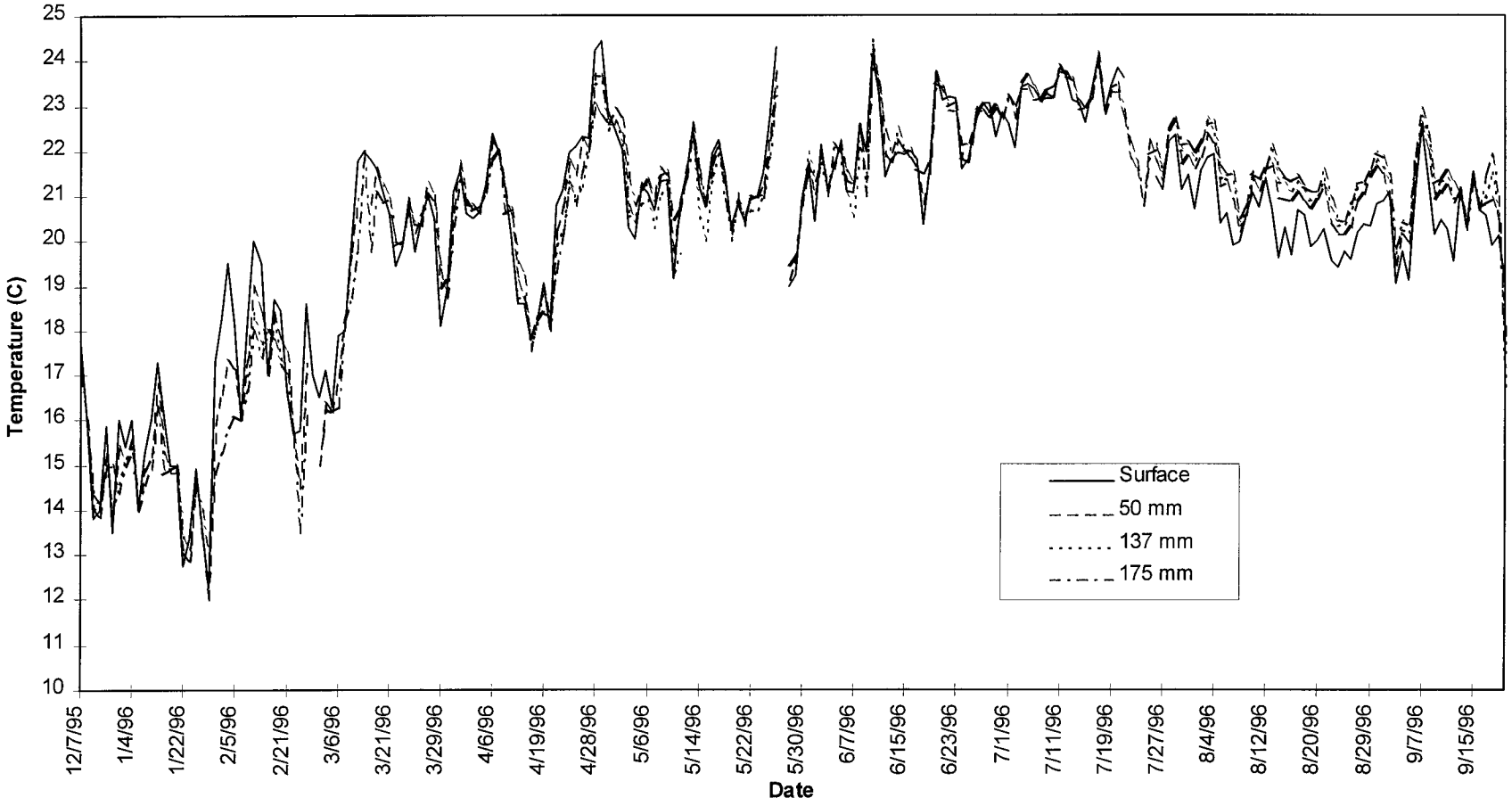

Figure 3.2 Daily average temperatures at surface and various in-depth positions

3.2 RAINFALL AND WATER CONTENTS OF UNTREATED MATERIALS

Figure 3.3 shows the monthly rainfall from July 1994 to November 1996 as recorded by the National Weather Service at Richmond, California (near the Richmond Field Station). Larger amounts of rain fell during the period from November 1994 through March 1995, just prior to the construction of the test sections. Little rainfall occurred during the period in which Section 500RF was tested; thus one might anticipate some drying of the sections. However, no tests were performed to show that the in-situ moisture contents of the untreated materials were lower at the beginning of HVS testing of Section 502CT than during testing of Section 500RF. Water content measurements made at the end of the Goal 1 tests in February 1997 were within the range of water contents observed at the start of the test program in April 1995, Table 3.4. It would appear that on the average, the subgrade was somewhat drier and that the water contents of base and subbase materials likely were about the same.

Table 3.4 Water contents

LOCATION	IN-SITU WATER CONTENT	
	March / April 1995[a]	February 1997[b]
aggregate base	4.2–6.0%	4.6–4.9%
aggregate subbase	4.0–7.9%	5.3–6.0%
subgrade	13.6–23.9%	14.4–16.3%

[a] water content tests conducted on twelve samples per layer
[b] water content tests conducted on four samples per layer

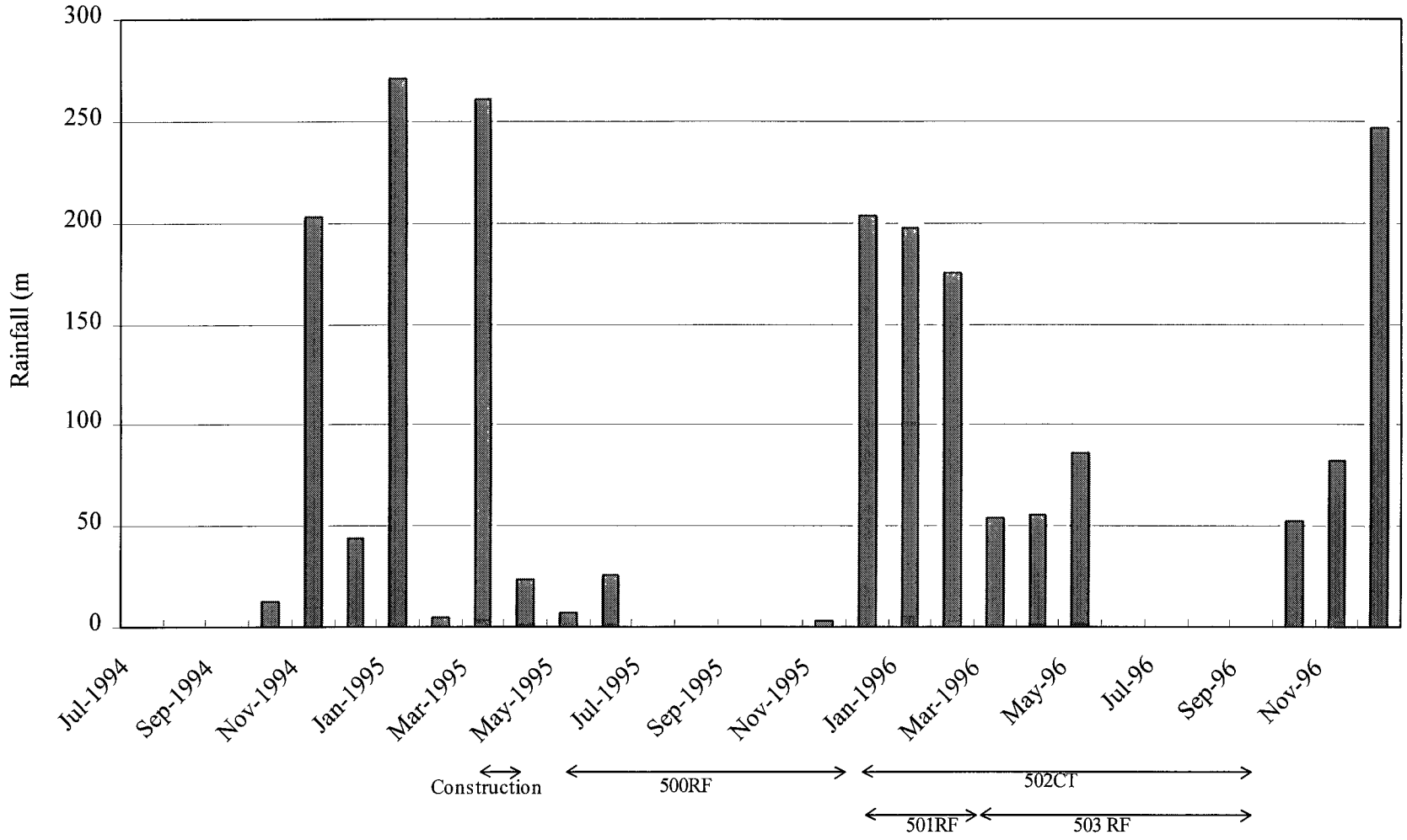

Figure 3.3 Monthly rainfall data in Richmond (National Weather Service)

3.3 PERMANENT DEFORMATION

Permanent deformations at the pavement surface were monitored with a laser profilometer and with multidepth deflectometers both at the surface and at various depths within the pavement. This section represents a summary of the results of both types of measurements.

3.3.1 Permanent Surface Deformation

Figure 3.4 shows the development of permanent deformation of the pavement surface versus the number of load repetitions as determined with the laser profilometer. These deformations were determined from transverse surface profiles obtained at each longitudinal position (every half meter) in the test section. Both the average rut and maximum rut depths are shown. Reference *(3)* describes how these were determined.

Figures 3.5 through 3.11 illustrate the development of rutting at different stages of loading. At 10,000 repetitions, the pavement surface exhibits negligible rutting, Figure 3.5; the deformations shown are likely irregularities existing prior to trafficking. Figures 3.6 to 3.11 show the increase in rutting from 150,000 up to 2.67 million repetitions. At the conclusion of trafficking (2.67×10^6 repetitions), the average rut was 9.8 mm while the average maximum rut was 13.7 mm, Figure 3.4. The most severe rutting occurred between Stations 10 and 16. The maximum rut, about 16 mm, occurred at Point 11; the profilometer data for that point are shown in Figure 3.12.

At the conclusion of the test, rut depth measurements were taken with both the laser profilometer and a straight edge at each station. Figure 3.12 illustrates a reasonable correspondence between the two measurement methods.

A comparison of rutting measured with the laser profilometer and the MD sensor at the surface at Point 4 is shown in Figure 3.13. Again, reasonable correspondence was obtained.

Figure 3.4 shows the variations that occurred in the rate of rut development throughout the test. To characterize stages with different rates of rut development during the life of the pavement, the data presented in this figure were divided into phases determined from changes in the loading and the visually apparent changes in the rate of permanent deformation. These phases are shown in Table 3.5 with calculated rutting rates expressed in millimeters of rut per million load applications (mm/MiLA).

Table 3.5 Rutting rates during HVS loading on Section 502CT determined from profilometer measurements

Phase	Repetitions ($\times 10^3$)	Load (kN)	Condition	Average Rut (mm)	Maximum Rut (mm)	Rut Rate[a] (mm/MiLA)
I	0 - 40	40	Embedding	1.2	1.8	29.7
II	40 - 150	40	Steady-State	1.5	2.2	2.7
III	150 - 200	80	Embedding	2.3	3.3	20.0
IV	200 - 350	100	Embedding	4.1	5.8	11.6
V	350 - 1300	100	Transition	7.2	10.1	3.3
	1300	100	Cracking	x	x	—
VI	1300 - 2100	100	Steady-State	8.8	12.9	1.9
VII	2100 - 2674	100	Steady-State	9.4	13.7	1.1

[a] MiLA = Million Load Applications

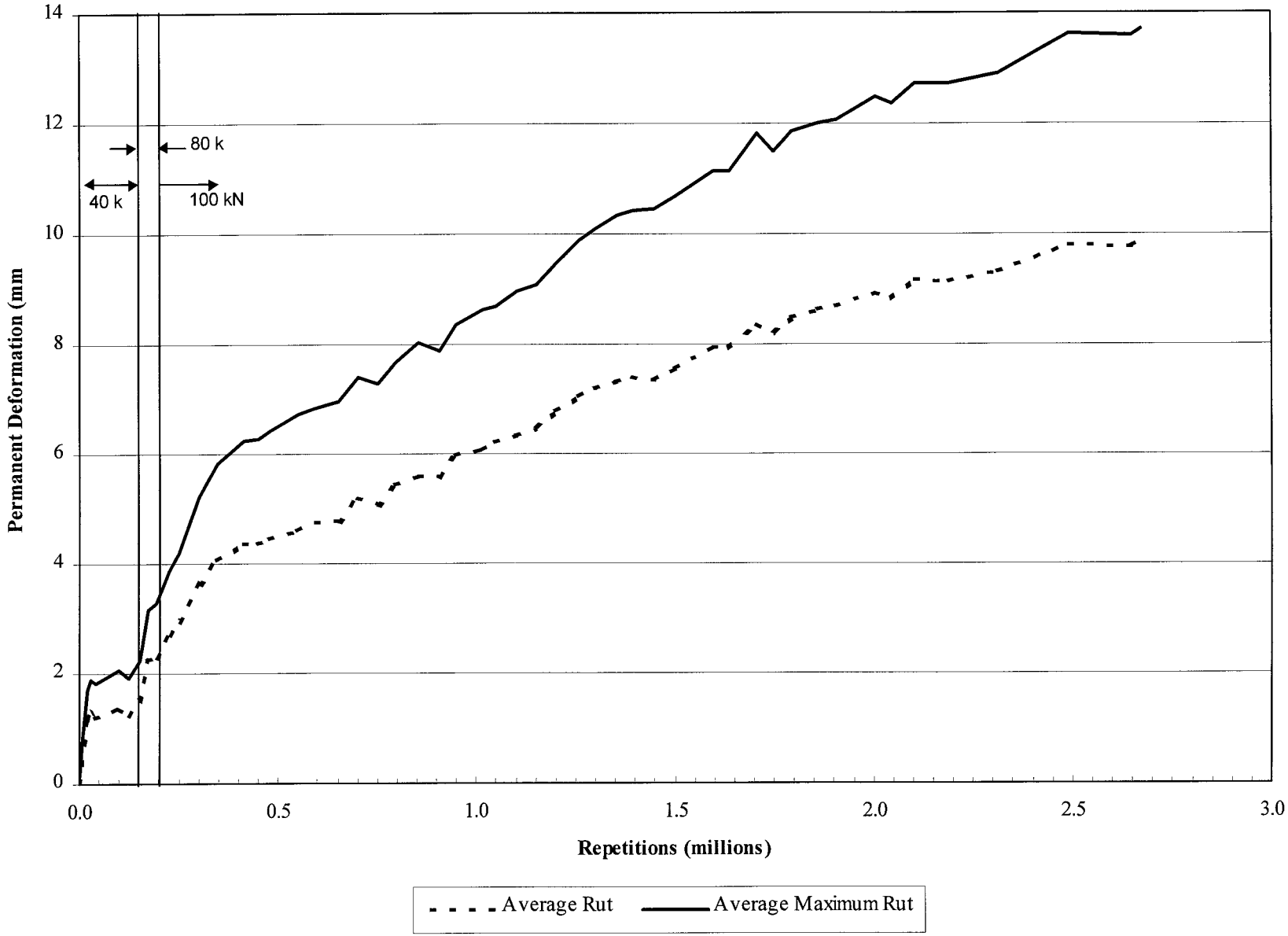

Figure 3.4 Permanent deformation determined from laser profilometer

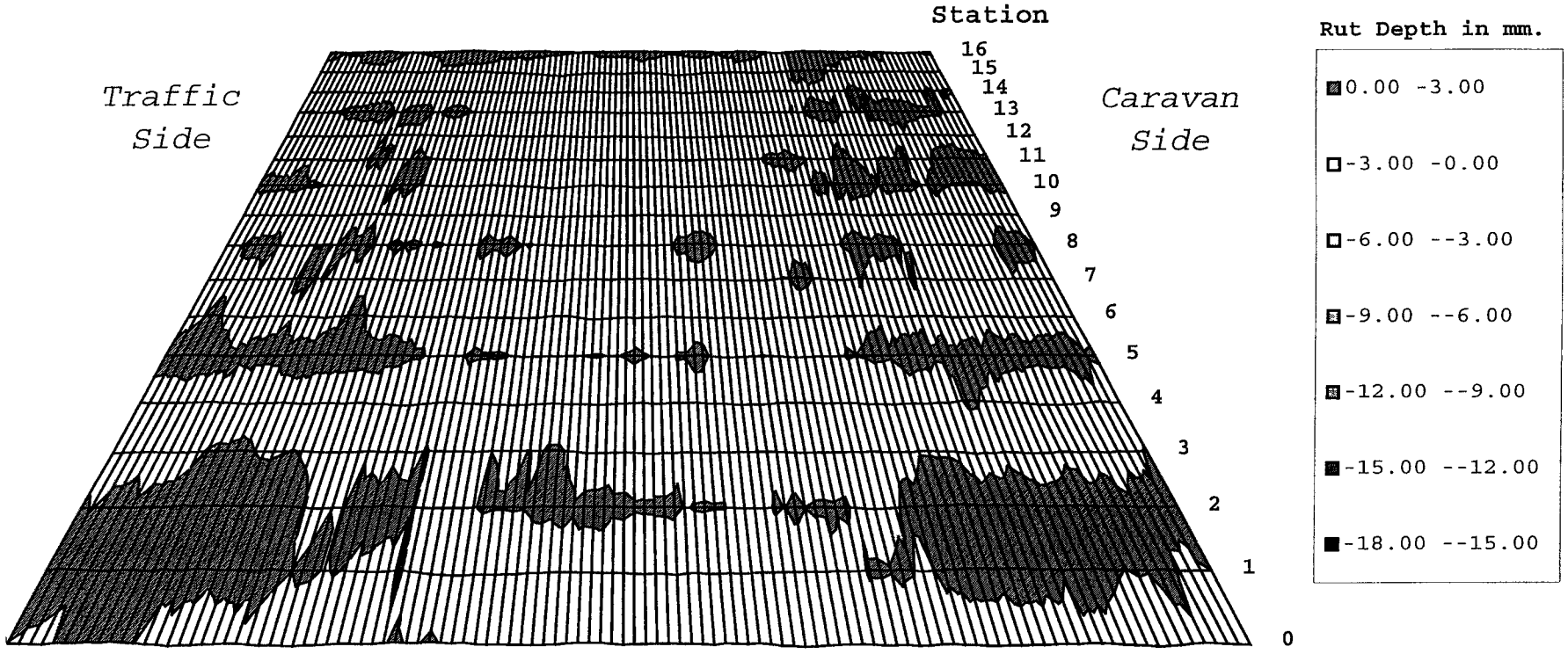

Figure 3.5 Surface permanent deformations at 10,000 repetitions

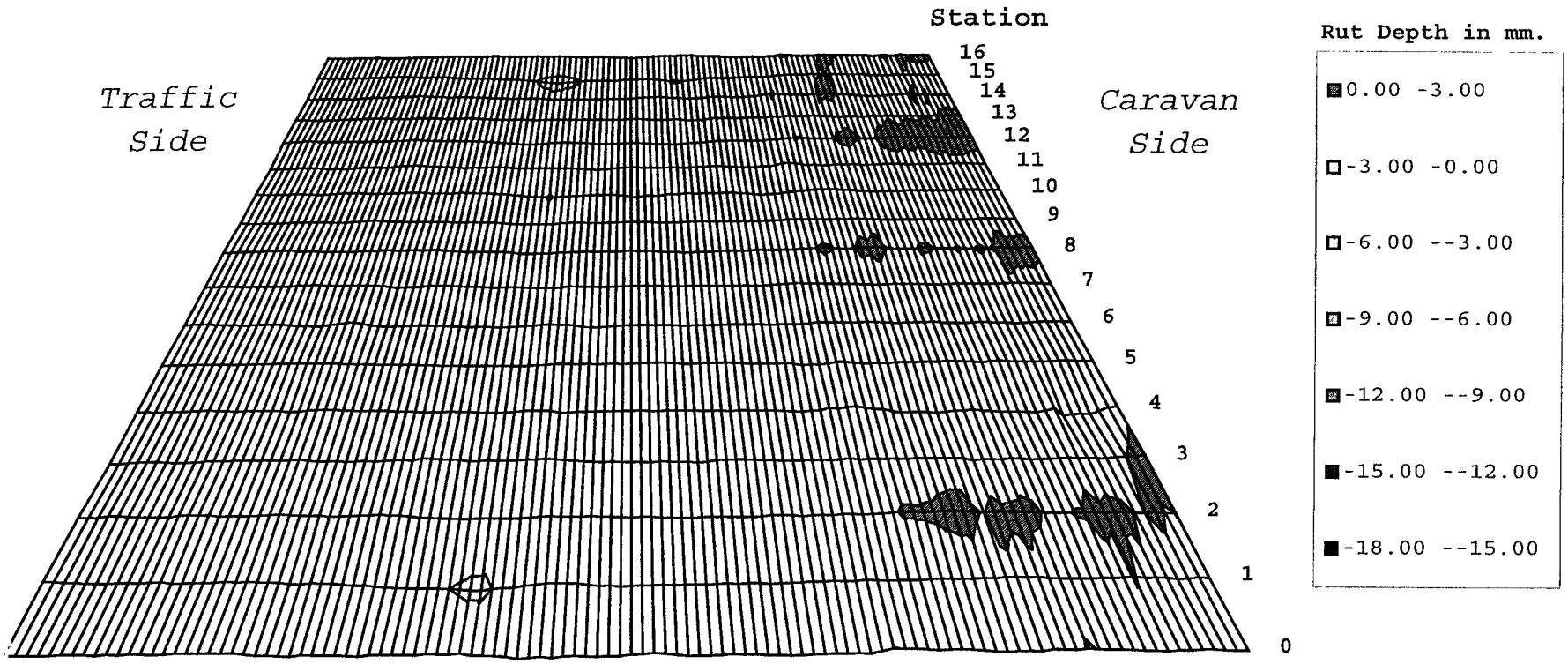

Figure 3.6 Surface permanent deformations at 150,000 repetitions

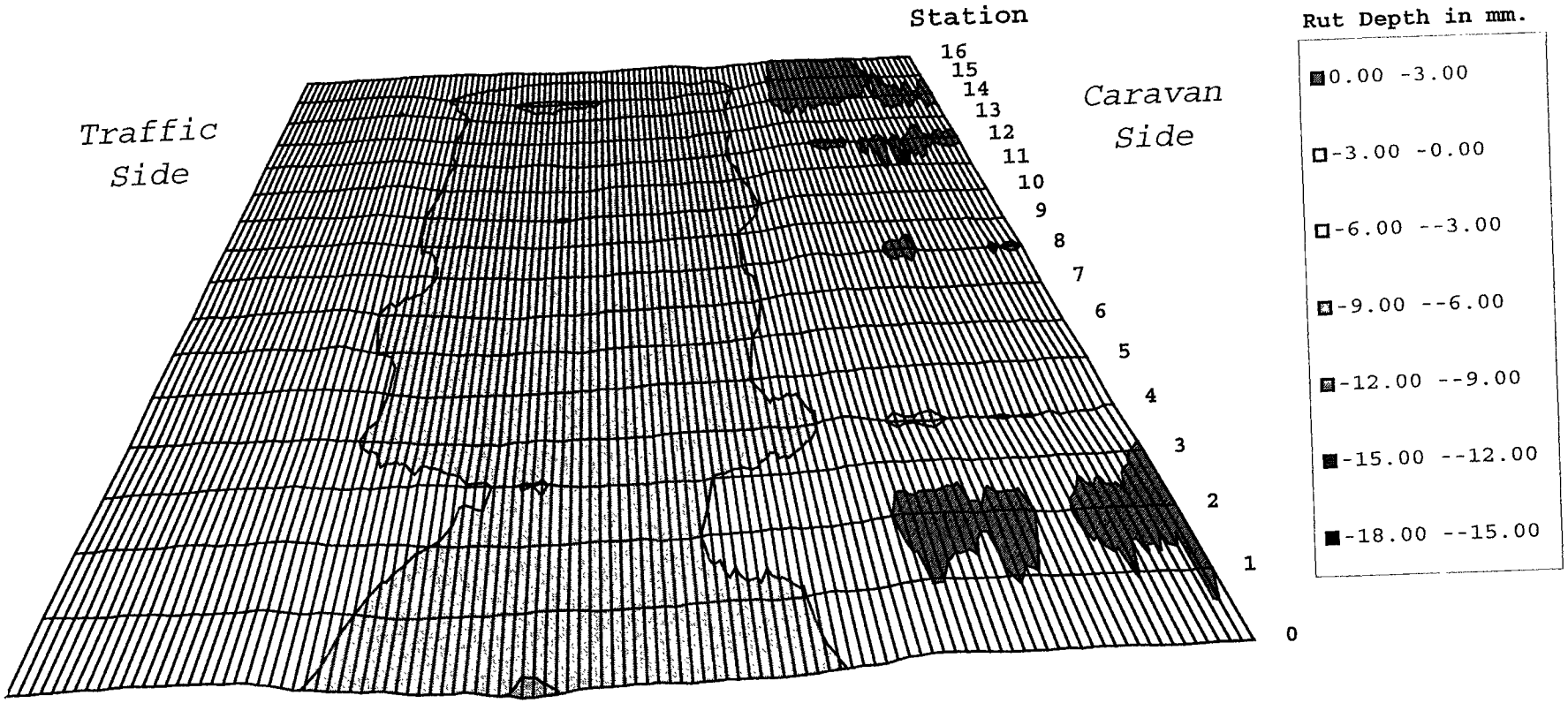

Figure 3.7 Surface permanent deformations at 300,000 repetitions

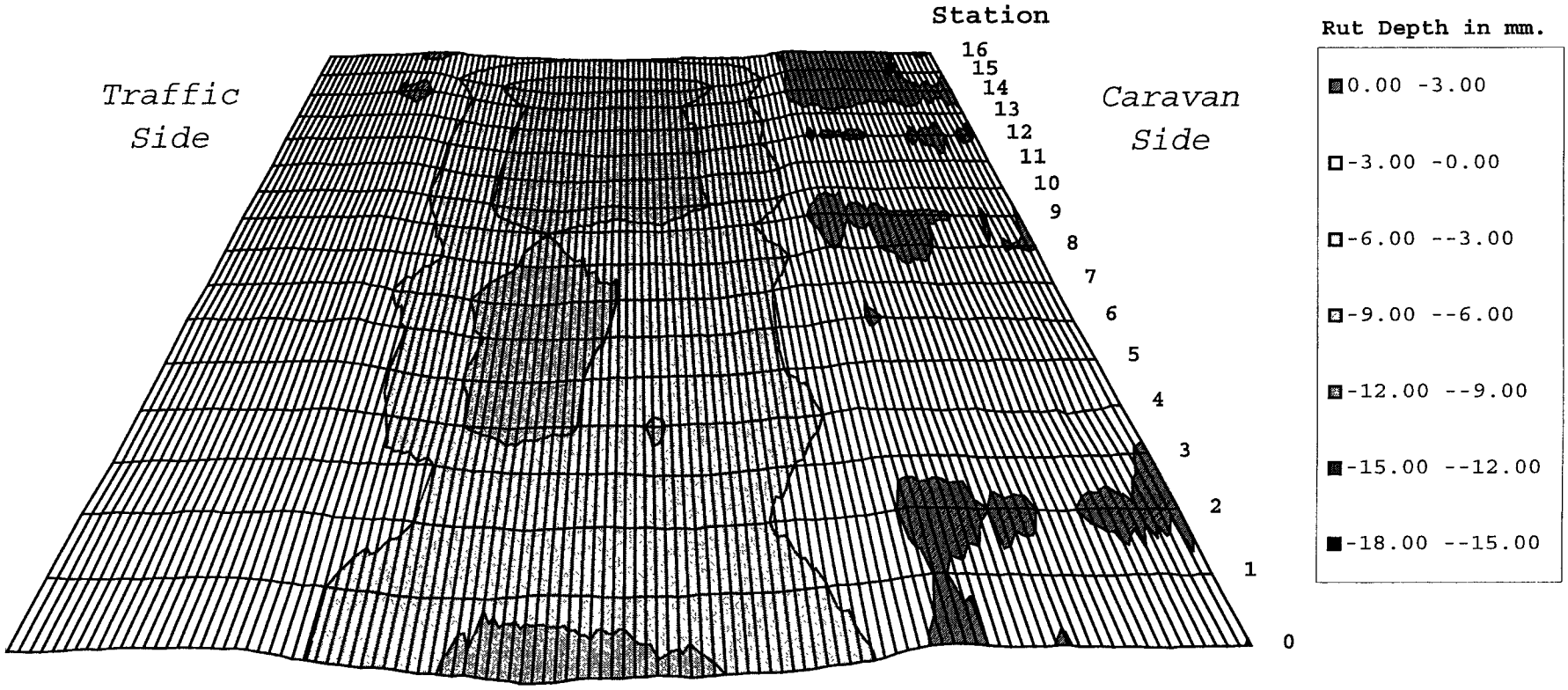

Figure 3.8 Surface permanent deformations at 600,000 repetitions

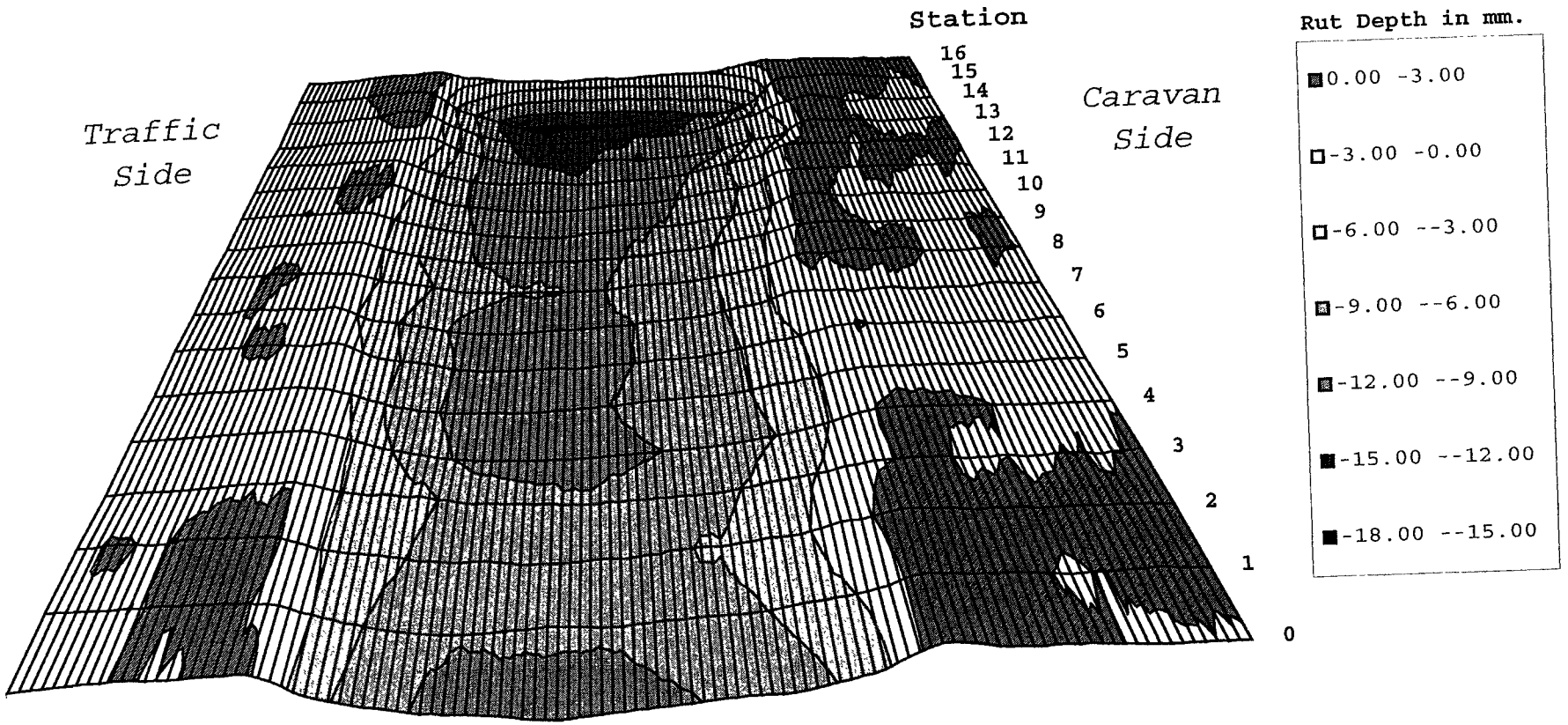

Figure 3.9 Surface permanent deformations at 1.5 million repetitions

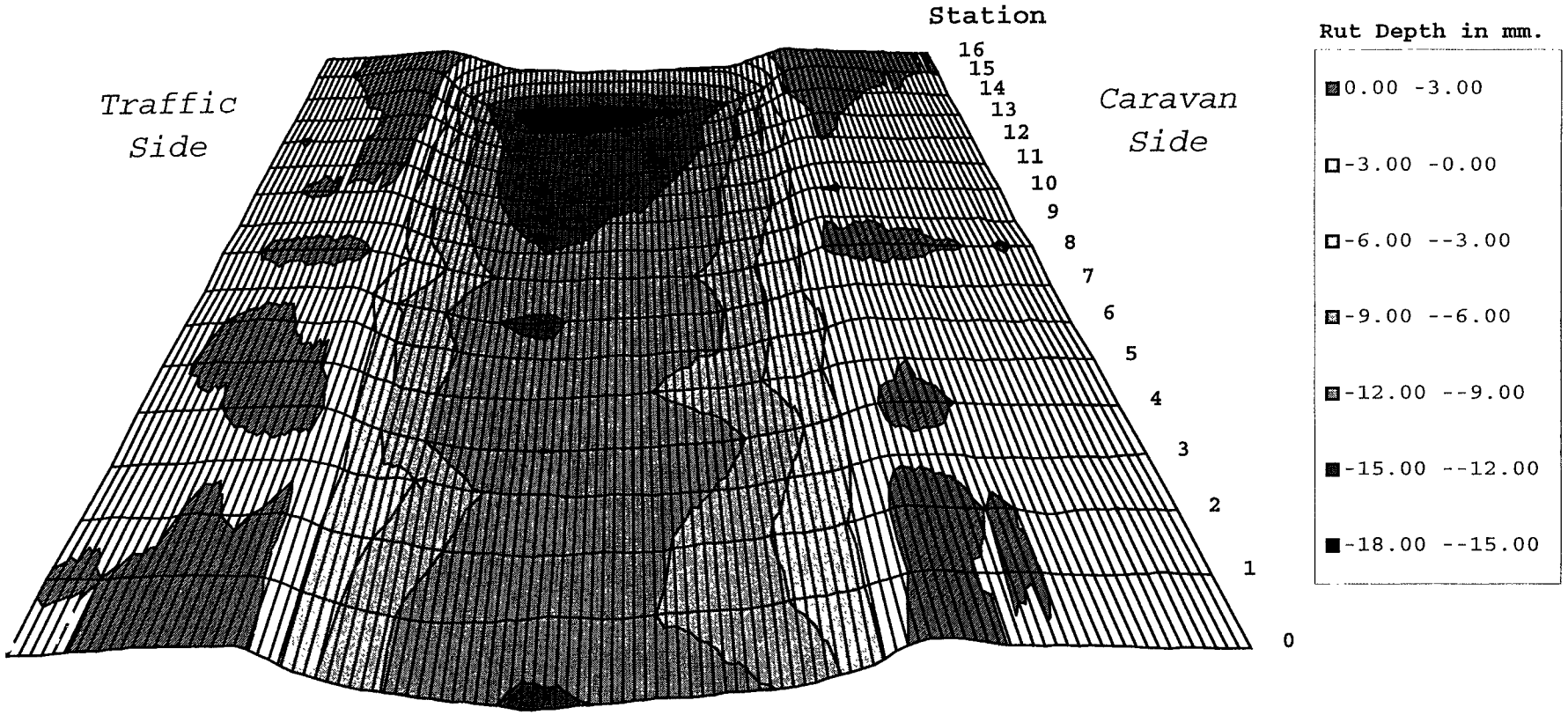

Figure 3.10 Surface permanent deformations at 2 million repetitions

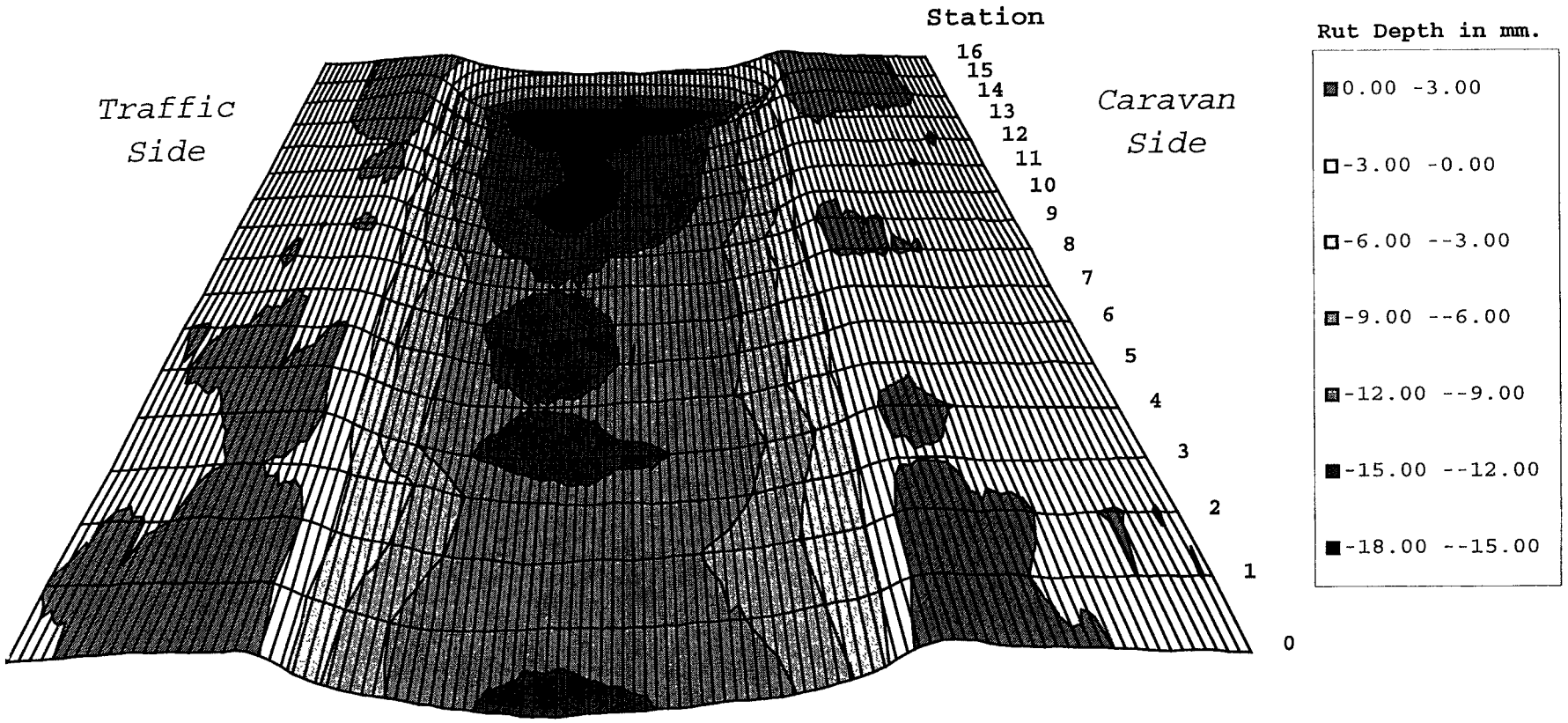

Figure 3.11 Surface permanent deformations at 2.67 million repetitions

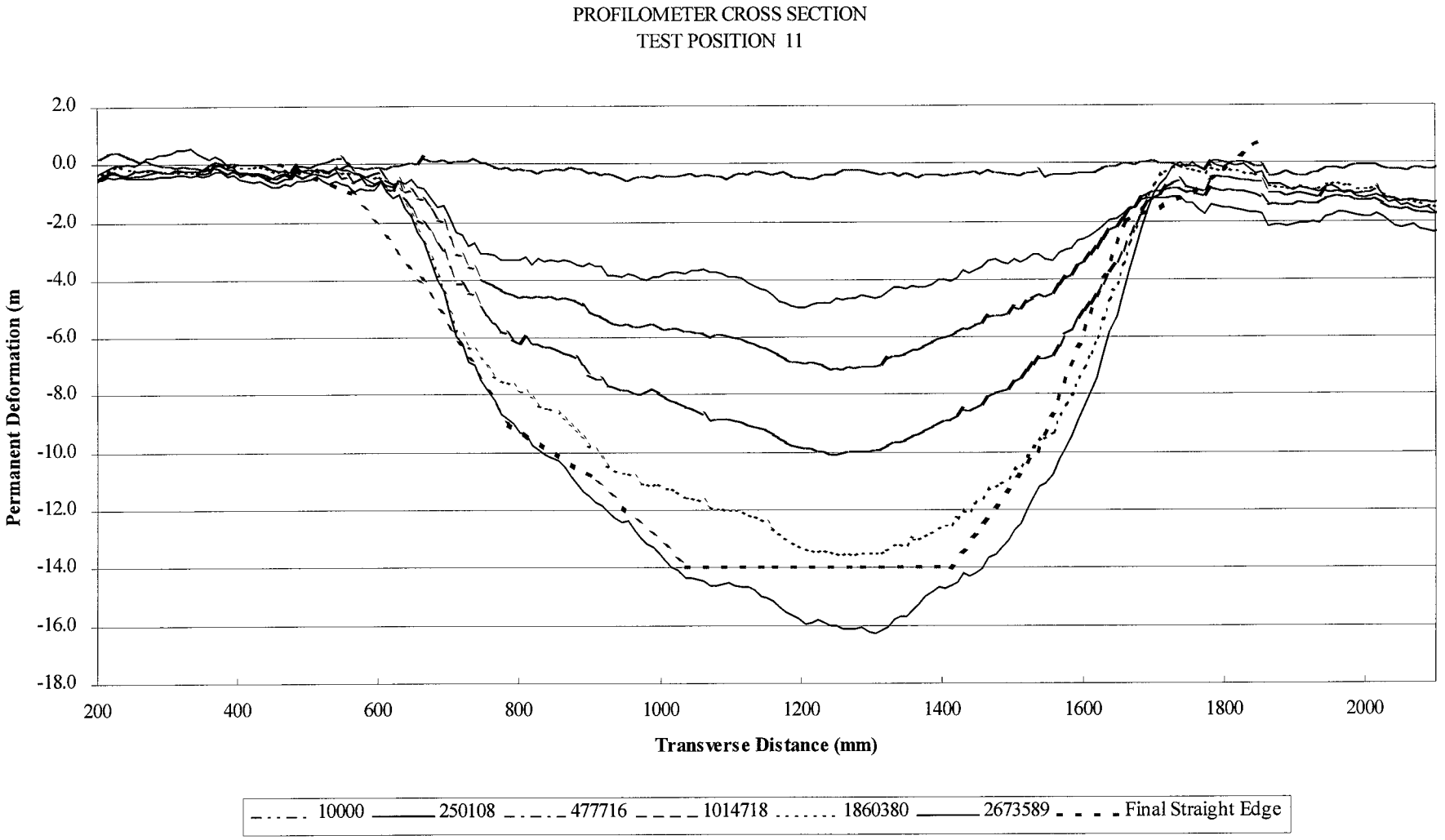

Figure 3.12 Profilometer cross section and straight edge measurements

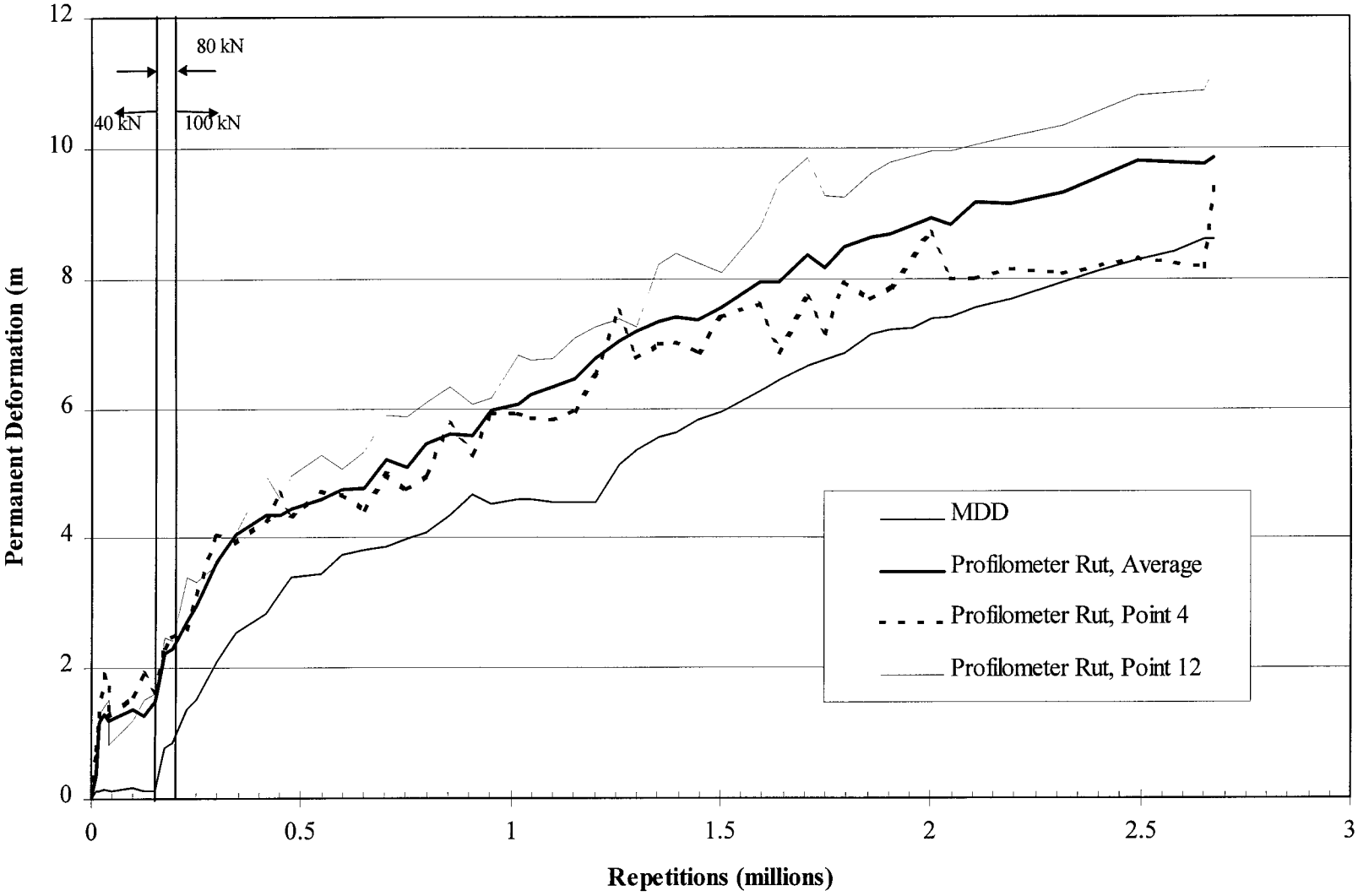

Figure 3.13 Comparison of permanent deformations measured with the MDD and the Laser Profilometer

The pattern of permanent deformation development from loading is similar to the previous three sections. The first phase, to 40,000 repetitions, is considered an embedding phase under the 40-kN load. After about 40,000 repetitions, the rutting rate decreased significantly. As with the earlier tests, however, the 40-kN load was maintained to 150,000 repetitions to ensure that the initial bedding phase was completed. When the load was increased to 80 kN and thence to 100 kN, additional embedding took place under each increase as seen in Figure 3.4 and in Table 3.5.

At 1,300,000 repetitions, cracking was observed at the pavement surface. However, the cracking did not influence the development of rutting as seen in Figure 3.4 and from the rut rate determinations shown in Table 3.5. It is interesting to note that at this number of repetitions, about 70 percent of the total permanent deformation observed at the end of the test had occurred.

3.3.2 In-Depth Permanent Deformation

Accumulation of permanent deformations with load repetitions as measured by the MDDs at Point 4 and 12 are shown in Figure 3.14. As seen in this figure, the data suggest some upward movement at the subgrade level. The reason for this is not known at this time. However, to provide a comparison of the permanent deformation data with the results of the other three tests, the decision was made to discard the test intervals in which negative permanent deformation readings were obtained. The values resulting from this adjustment are shown in Figure 3.15.

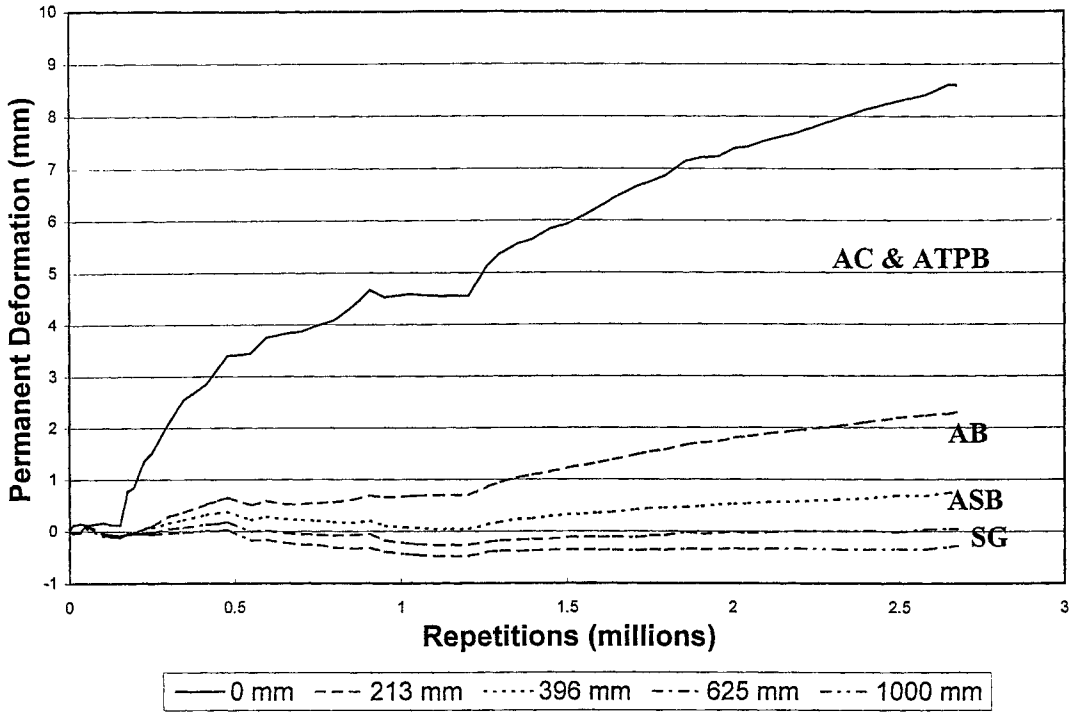

a. Point 4

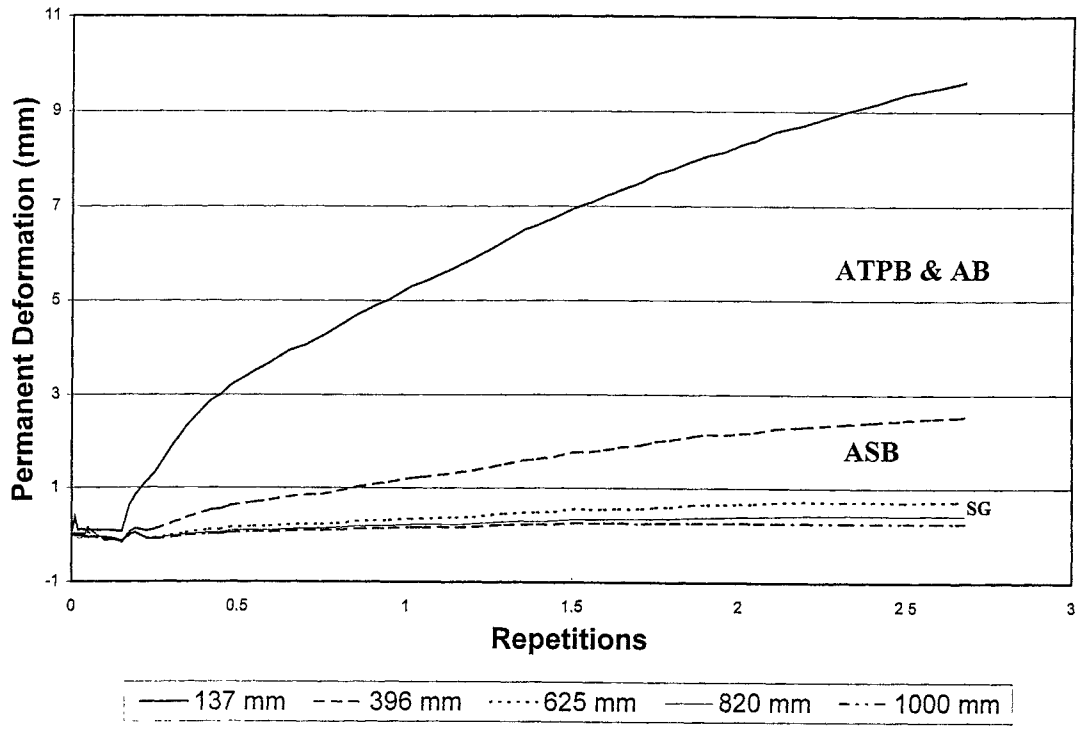

b. Point 12

Figure 3.14 Permanent deformations measured at MDD locations

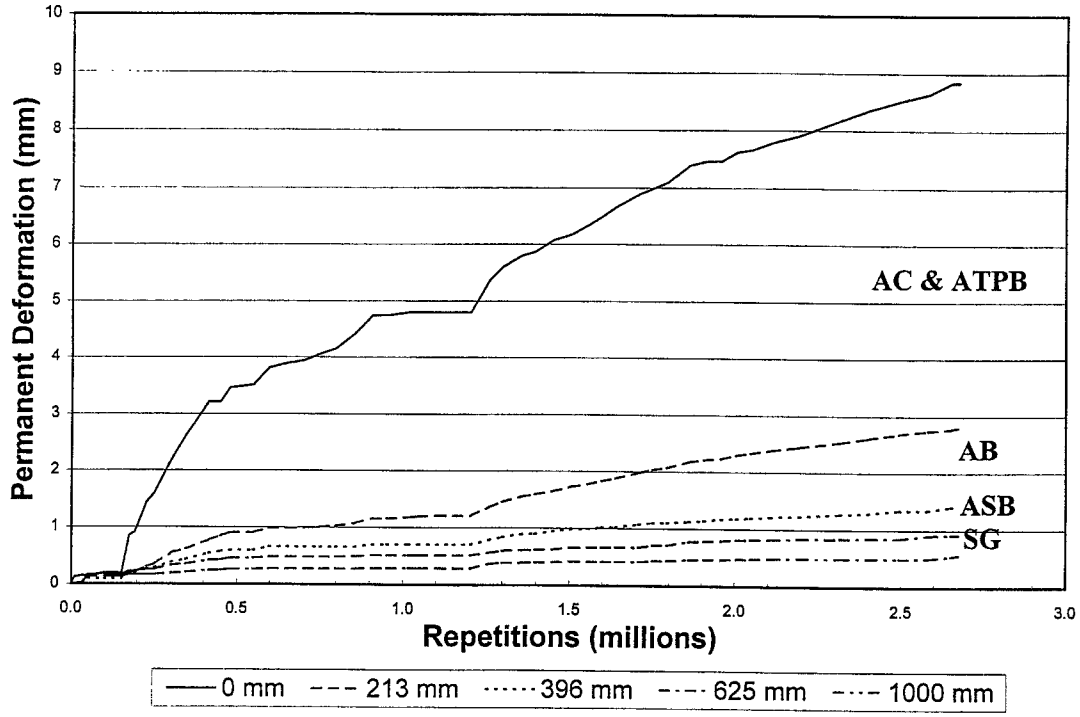

a. Point 4

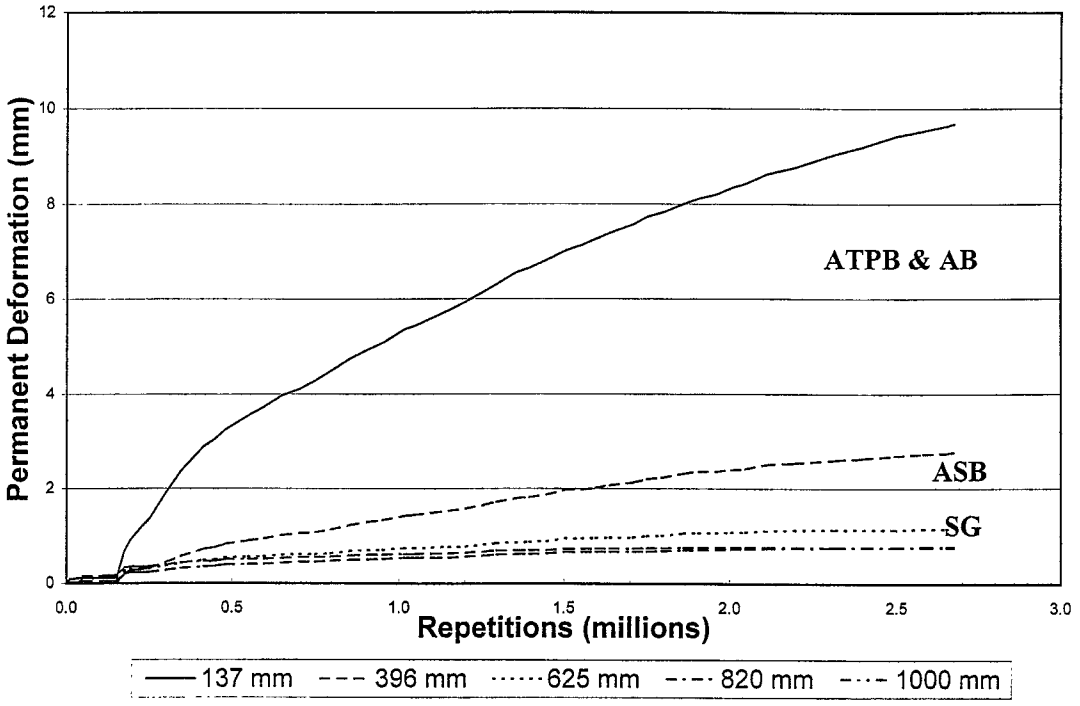

b. Point 12

Figure 3.15 Adjusted permanent deformations measured at MDD locations

With the values for permanent deformation shown in Figure 3.15, permanent deformations occurring in the various layers were determined and are summarized in Table 3.6.

The resulting deformations included in Table 3.6 were obtained as follows:

a. Subgrade, subbase, and untreated aggregate base deformations represent the average of MDD measurements for both Points 4 and 12.

b. The deformation in the asphalt concrete and asphalt-treated permeable base was obtained for the MDD measurements at Point 4.

The results in this table are compared with those from the 500RF test; it will be noted that similar performance in terms of permanent deformations in the various pavement components was obtained in both sections.

Table 3.6 Permanent deformations measured by MDD modules

Layer	Section 502CT			Section 500RF
	Nominal Thickness (mm)	Vertical Permanent Deformation (mm)	Percentage of Total Deformation	Percentage of Total Deformation
Asphalt Concrete	148	5.3	60.2	59
ATPB	76			
Aggregate Base	182	1.4	15.9	17
Aggregate Subbase	215	1.0	11.4	12
Subgrade	semi-infinite	1.1	12.5	12
Total		8.8	100	100

3.3.2.1 Asphalt layers

Table 3.6 shows that the asphalt concrete plus ATPB layers contributed about 60 percent of the observed surface permanent deformation in the vicinity of Point 4 which is about the same as that for Section 500RF, results for which are also summarized in this table.

In Figures 3.9 through 3.11 it will be noted that permanent deformations, as measured by the laser profilometer, increased somewhat in the direction from Point 4 to Point 12. Also, as seen in these figures, as well as in Figure 3.12, there was relatively little upheaval of the asphalt concrete adjacent to the rutted area.

To determine the densification which took place during HVS loading, four 150-mm diameter cores were extracted from the test pavement. Two cores were obtained within the area subjected to trafficking while the other two were obtained from the untrafficked portion. The results of air void determinations in these cores are summarized in Table 3.7.

Table 3.7 Air-void contents in the asphalt concrete layer

	Specimen	% Air Voids Top Lift	% Air Voids Bottom Lift
Outside Trafficked Area	1	7.5	3.4
	2	7.6	4.5
	Average	7.6	4.0
Inside Trafficked Area	15	5.9	2.2
	15.5	4.5	2.2
	Average	5.2	2.2

From the data presented in Table 3.7, it is apparent that some densification of the asphalt concrete in both lifts occurred from the HVS trafficking. The top lift exhibited a 2.4 percent reduction in air voids while the bottom lift showed a 1.8 percent decrease. For volume

changes of these magnitudes, it would be anticipated that the amount rutting in the asphalt concrete related to the reduction in air voids should not exceed about 1.5 mm *(10)*. Accordingly, the remaining amount is likely due to shear (deviatoric) deformations. While there is little upheaval at the edge of the ruts, e.g. Figure 3.12, experience with the other test sections suggests that the rutting in the asphalt concrete results primarily from the shear deformations in the upper portion of the asphalt concrete. Trenching of the sections after the completion of the HVS tests on the overlay pavement should provide a more definitive indication of the cause of the permanent deformation in the asphalt concrete (and ATPB) layer.

3.3.2.2 Aggregate Base

Permanent deformation in the aggregate base was determined from MDD measurements at Point 4. As seen in Table 3.6, about 16 percent of the total deformation occurred in this layer. As noted from the information contained in this table, the aggregate base layer in Section 502CT performed similarly to the same base in Section 500RF.

3.3.2.3 Aggregate Subbase and Subgrade

The permanent deformation in the subbase, about 11 percent, was obtained by averaging the results of the MDD measurements from Points 4 and 12. This amount of permanent deformation corresponds to that obtained in the subbase in Section 500RF. The data for the subgrade was obtained in the same manner. Table 3.6 indicates that the permanent deformations in both Sections 502CT and 500RF were about the same. The results show that the overall pavement thickness was adequate to minimize subgrade rutting, even under 100-kN loads for the temperature conditions of this test.

3.4 ELASTIC DEFLECTIONS

Elastic (recoverable) deflections provide an indication of the overall stiffness of the pavement structure and, therefore, a measure of load carrying capacity. The stiffness of a structure decreases as damage occurs, resulting in an increase in deflection for a given load and tire pressure. During HVS testing, elastic deflections are measured with two instruments: the multi-depth deflectometer (MDD) and the road surface deflectometer (RSD). The RSD measures surface deflection basins whereas the MDD measures the surface deflections at Point 4 and in-depth deflections at both Points 4 and 12.

3.4.1 Surface Deflections

In this section, surface deflections as measured by the RSD and the MDD at Point 4 versus load repetitions are summarized. Since the temperature did not vary significantly during the test, the influence of temperature on the deflections measured by the RSD was not determined.

3.4.1.1 RSD Surface Deflection Results

Figures 3.16a and 3.16b show the individual RSD deflections for centerline measuring Points 2, 6, 8, 10, and 12 under the 40-kN and 100-kN loads, respectively. With exception of Point 12, the deflections are all within a narrow band indicating uniform structural behavior for the majority of the test section. As seen earlier, the permanent deformation in the vicinity of Point 12 was larger than that elsewhere within the test section, suggesting a somewhat weaker area there; the elastic deflections at this point support the other observations. The variations

between the centerline deflections at Points 4, 6, 8, and 10 is approximately 15 percent throughout the testing period.

Average 40-kN deflections for the centerline measurements are shown in Table 3.8 before HVS testing and after the completion of loading. The increase in deflection, 229 percent, is a significant change and is likely due to the cracking which developed in the asphalt concrete as loading progressed (described in Section 3.5).

Table 3.8 Average of 40-kN RSD deflections

	Before HVS testing	**After 2.67×10^6 HVS load applications**
Average deflection (microns)	267	878
Standard deviation	29	79

Average RSD deflections are illustrated in Figures 3.17a and 3.17b for 40-kN and 100-kN loads, respectively. Periods with similar trends in the rate of increase in elastic deflection are indicated on these figures by roman numerals. Period I identifies the initial 150,000 repetitions at 40 kN, Period II identifies the next 50,000 repetitions as the load was increased from 40 kN to 80 kN, and Period III identifies the period where the load was increased to 100 kN. The graph shows that for Periods I through III, damage rates increased each time the load was increased. During Period IV (from 400,000 to 1.3 million repetitions) there is a steady increase of damage prior to the crack appearing at the surface. Period V (from 1.3 to 2.0 million repetitions) marks the change in damage accumulation after crack appearance and as crack lengths increased. The rate of deflection increase appears to slow thereafter under continued 100-kN loading in Period VI (2.0 to 2.67 million repetitions).

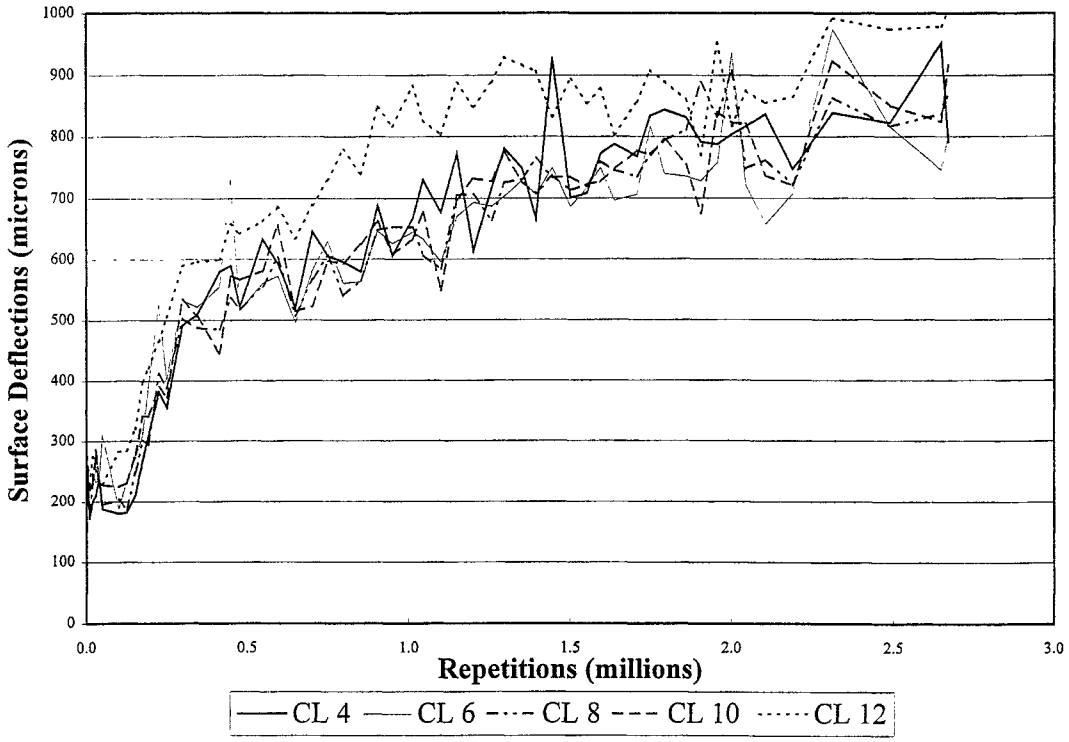

a. 40-kN test load

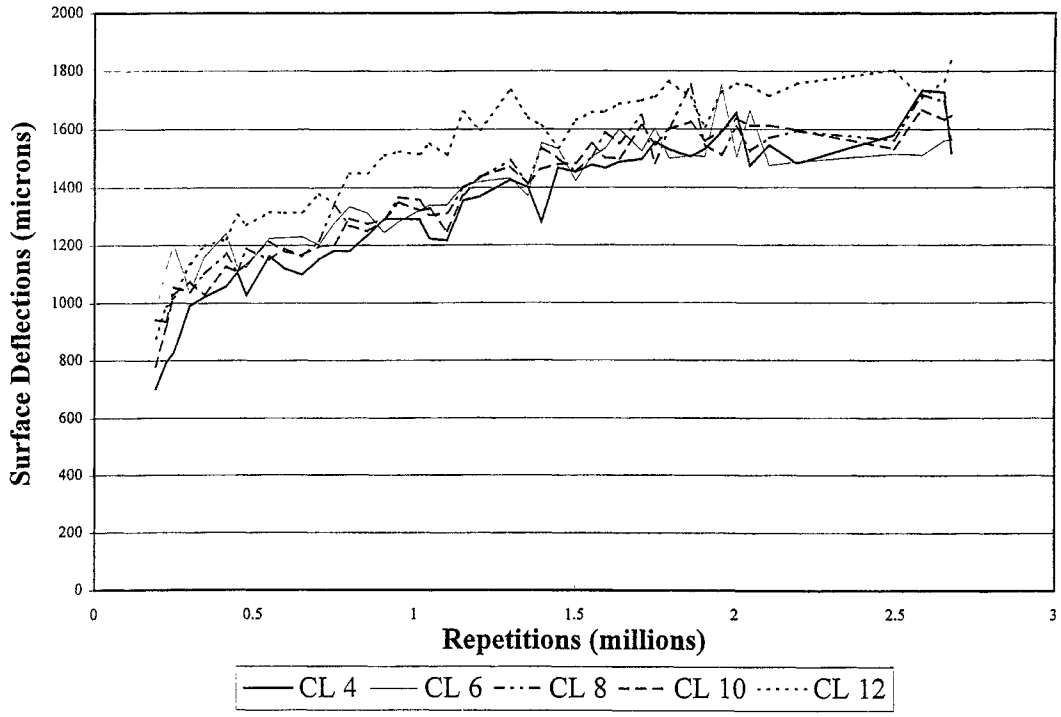

b. 100-kN test load

Figure 3.16 Road surface deflections from RSD measurements versus load applications

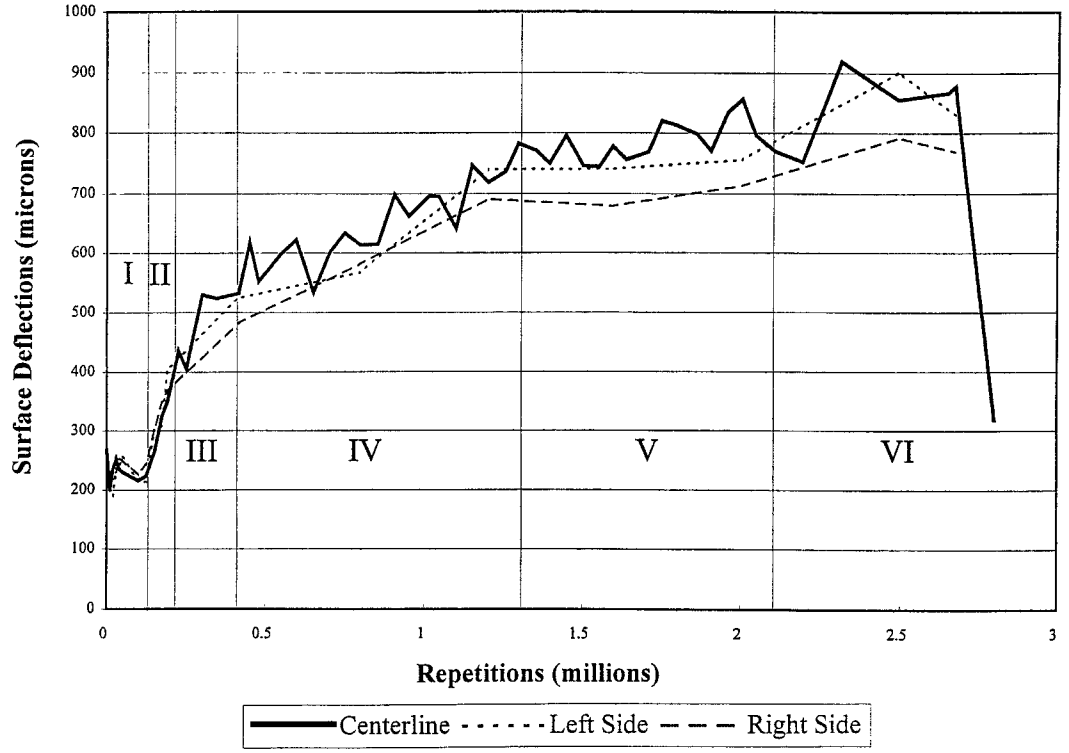

a. 40-kN test load

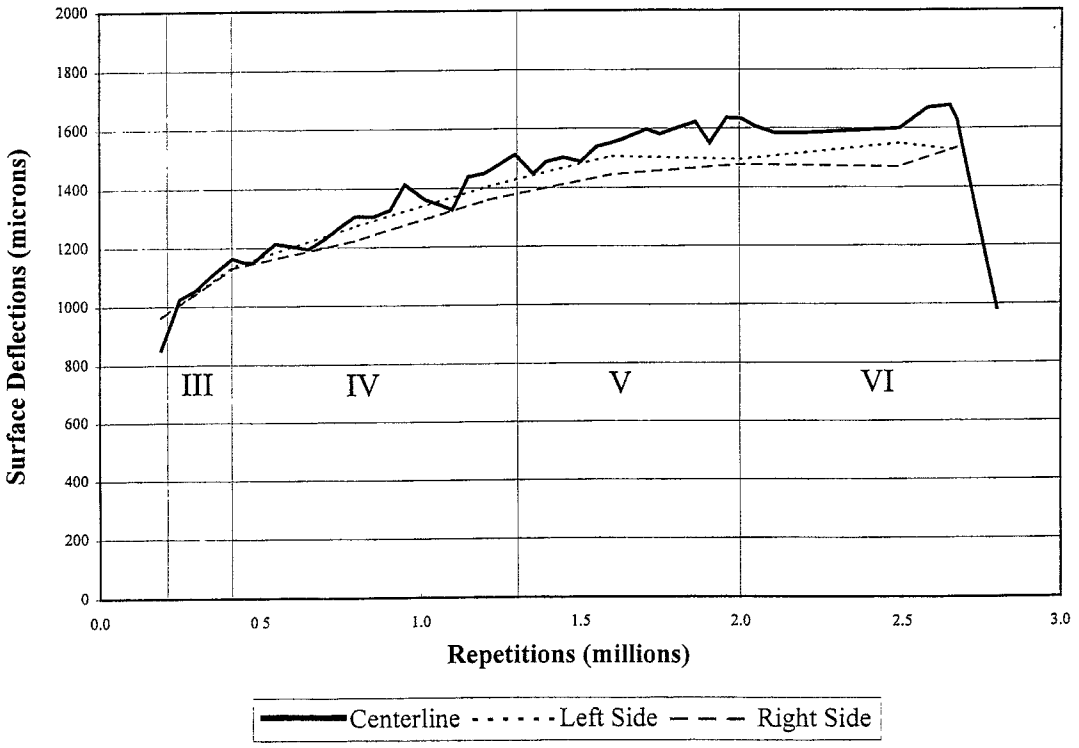

b. 100-kN test load

Figure 3.17 Average road surface deflections from RSD measurements versus load applications

3.4.1.2 MDD Surface Deflection Results

Figures 3.18a and 3.18b summarize the surface deflections measured by the MDD at Point 4 using the 40-kN and 100-kN loads respectively. Also shown in these figures are the results of the average RSD deflections measured at this point at the same time. Similar trends are visible between the two instruments and they are in agreement at the beginning of the test. As damage continues and deflections increase, the MDD measured less deflections than did the RSD. This data emphasizes the usefulness of the RSD data in defining the uniformity or lack thereof in the pavement structure and performance throughout the 1 by 8 m test sections, as well as providing an independent check of MDD measurements.

3.4.2 In-Depth Elastic Deformations

Figures 3.19a and 3.19b summarize the in-depth deflections measured under the 40-kN load by the MDDs at Points 4 and 12, respectively. Figures 3.20a and 3.20b show the data for Points 4 and 12 under the 100-kN load. Averages of the elastic deflection data measured on Section 502CT are summarized in Table 3.9 for the 40-kN and Table 3.10 for the 100-kN test loads. Table 3.9 shows the deflections under the 40-kN load at the time HVS loading commenced and after 2.67 million load applications. Table 3.10 shows the deflections for the 100-kN test load at 200,000 load repetitions, the point the traffic load was increased to 100 kN, and after 2.67 million load applications data contained in the these tables represent the average of three deflection measurements per measuring point.

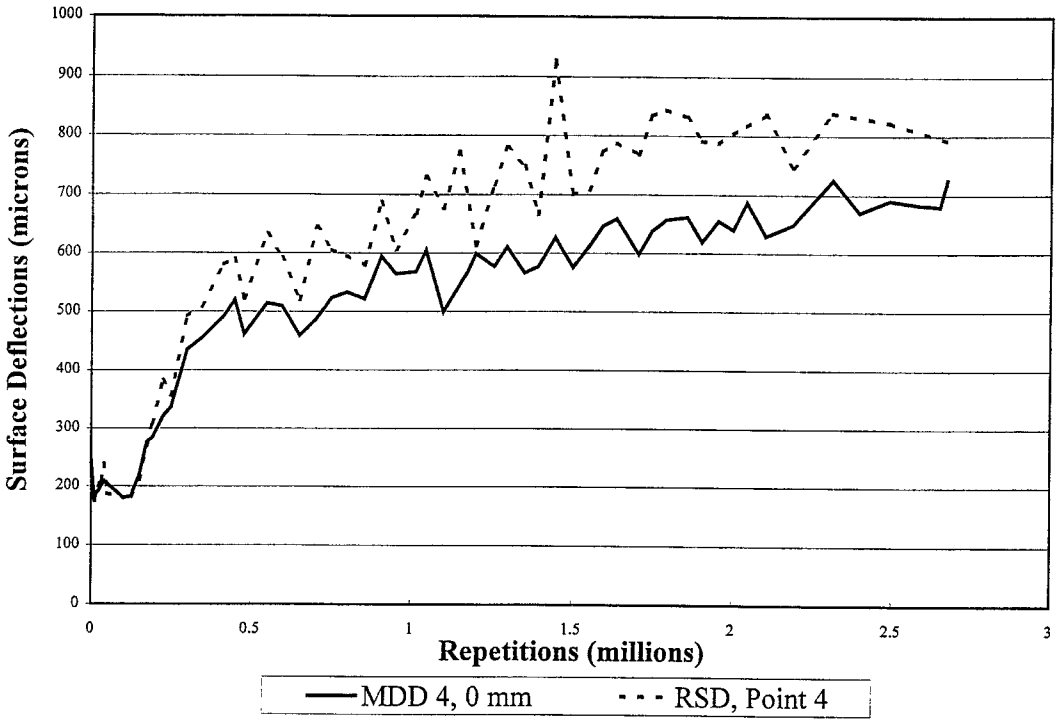

a. 40-kN load

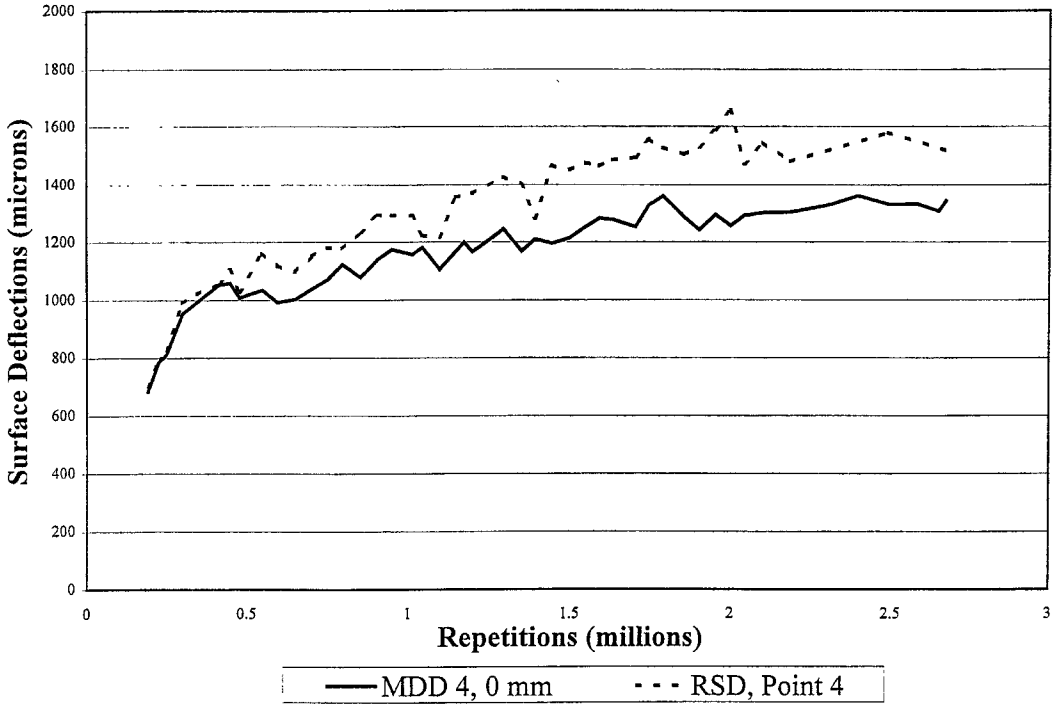

b. 100-kN load

Figure 3.18 Comparison of elastic deflections determined by the RSD and by the MDD at Point 4

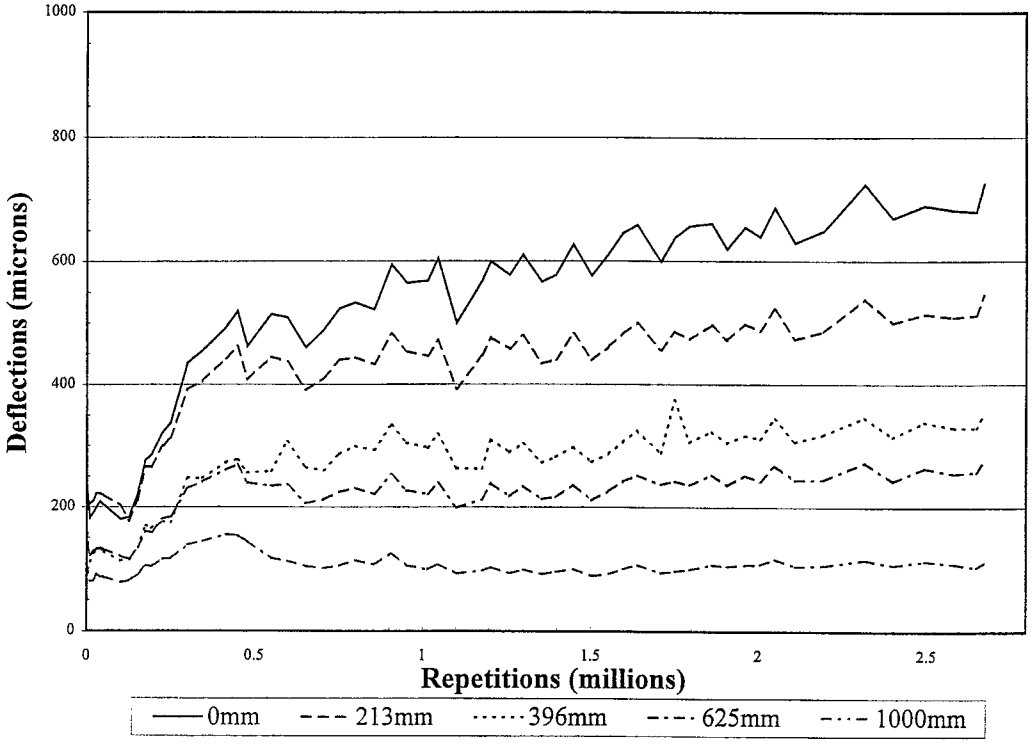

a. Point 4

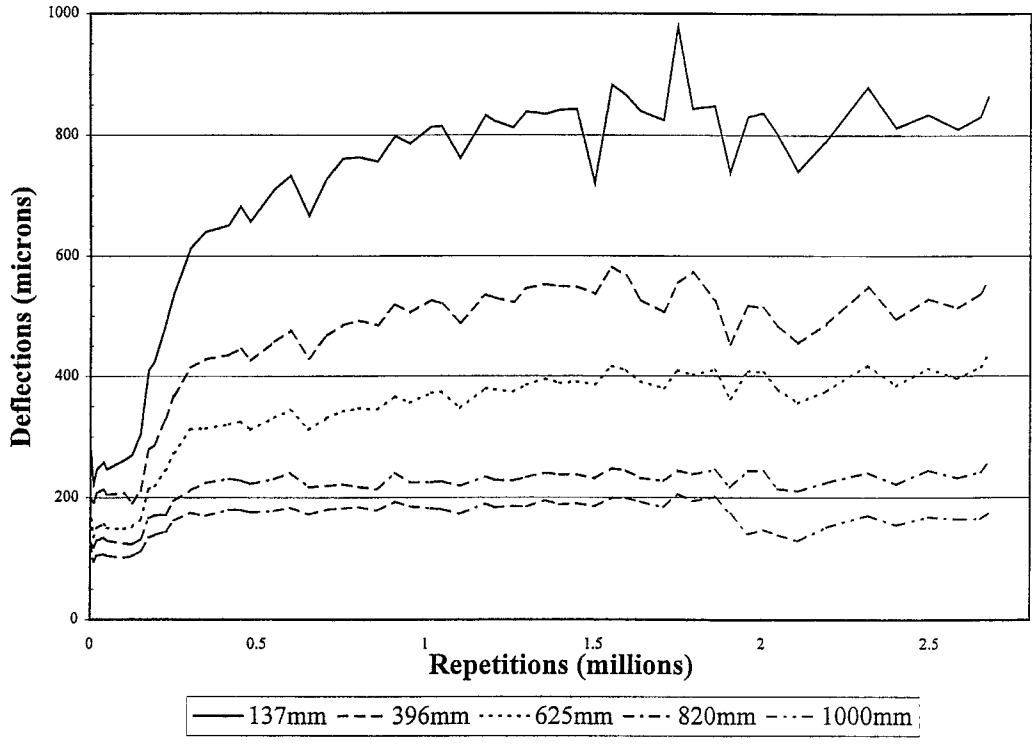

b. Point 12

Figure 3.19 Measured MDD deflections versus load repetitions at various depths below pavement surface, 40-kN test load

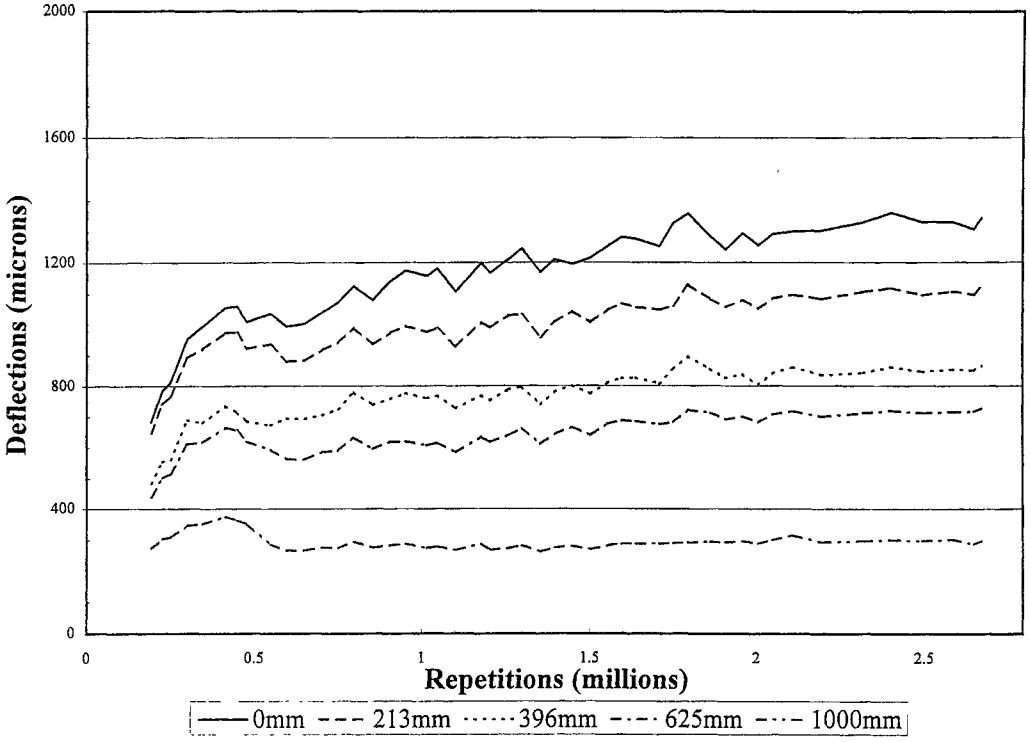

a. Point 4

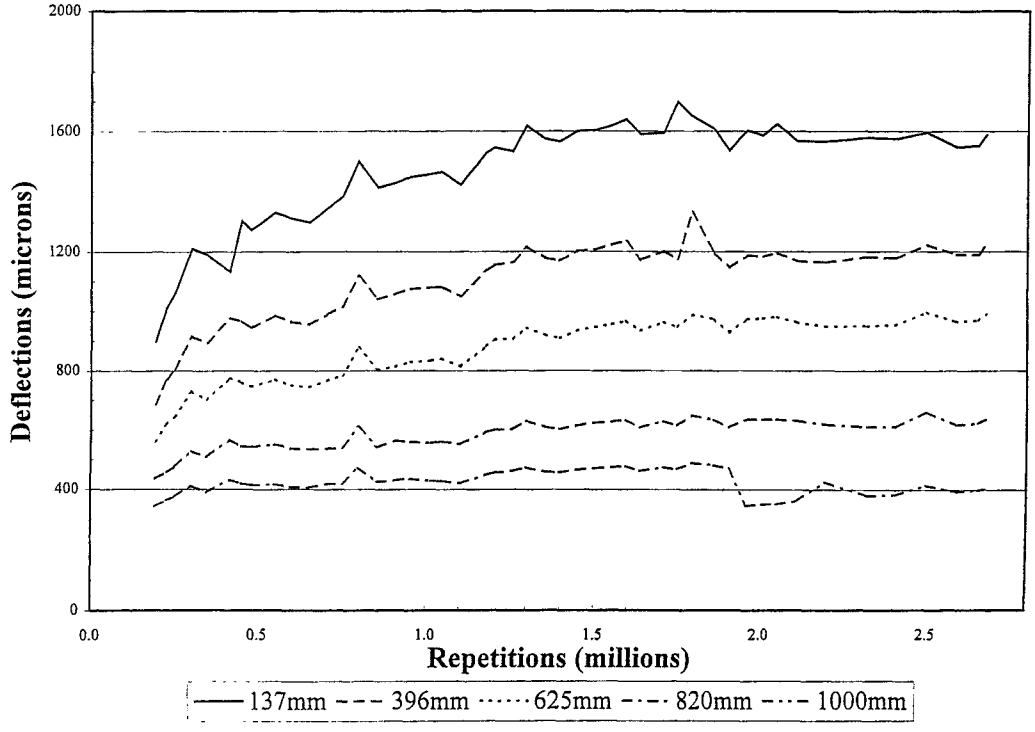

b. Point 12

Figure 3.20 Measured MDD deflections versus load repetitions at various depths below pavement surface, 100-kN test load

Table 3.9 Summary of 40-kN MDD elastic deflections

Level (mm)	Pavement Layer	Elastic in-depth Deflections (microns): Test Load = 40 kN			
		MDD at Point 4		MDD at Point 12	
		Before HVS loading	After 2.67 M load applications	Before HVS loading	After 2.67 M load applications
0	AC	238	726	NA	NA
137	ATPB	NA	NA	285	864
213	AB	213	546	NA	NA
396	ASB	172	352	200	559
625	SG	143	275	180	434
820	SG	NA	NA	128	257
1000	SG	107	112	127	174

NA MDD modules were not placed at these locations (see Figure 2.2)

Table 3.10 Summary of 100-kN MDD elastic deflections

Level (mm)	Layer	Elastic in-depth Deflections (microns): Test Load = 100 kN			
		MDD at Point 4		MDD at Point 12	
		After 200k load repetitions	After 2.67 M load repetitions	After 200k load repetitions	After 2.67 M load applications
0	AC	684	1342	NA	NA
137	ATPB	NA	NA	898	1587
213	AB	646	1122	NA	NA
396	ASB	484	866	686	1222
625	SG	439	726	561	989
820	SG	NA	NA	436	635
1000	SG	273	299	342	401

NA MDD modules were not placed at these locations (see Figure 2.2)

It can be seen in Tables 3.9 and 3.10 that the largest changes in deflection during loading occurred in the asphalt concrete lifts.

The proportion of the surface deflection each layer contributed to the total can be calculated from the deflection results presented in Tables 3.9 and 3.10. Results of these determinations are shown in Tables 3.11 and 3.12 for the 40-kN and 100-kN test loads, respectively.

Table 3.11 Percentage elastic deflection per layer, 40-kN test load

Pavement Layer	Percentage of total elastic deflection			
	MDD at Point 4		MDD at Point 12	
	Before HVS loading	After 2.67 M load applications	Before HVS loading	After 2.67 M load applications
AC/ATPB	10.5	24.8	NA	NA
ATPB/AB	NA	NA	29.8	35.3
AB	17.2	26.7	NA	NA
ASB	12.2	10.6	7.0	14.5
SG	60.1	37.9	63.2	50.2

NA MDD modules were not placed at these locations (see Figure 2.2)
Note: Calculated from Table 3.9

Comparisons of the data from Tables 3.11 and 3.12 with the corresponding data from Test Section 500RF show similar results for the MDD at Point 4 for proportions of the elastic deformations associated with the various layers for both the 40-kN and 100-kN loads. While the individual results for the untreated base and subbase differ, their sums correspond closely to those for the same materials in Test Section 500RF. The corresponding results for the MDD at Point 12 differ somewhat. Reasons for this must await the results obtained from trending studies to be conducted at the conclusion of the Goal 3 overlay tests on the four sections.

Table 3.12 Percentage elastic deflection per layer, 100-kN test load

Pavement Layer	Percentage of total elastic deflection			
	MDD at Point 4		MDD at Point 12	
	After 200k load applications	After 2.67 M load applications	After 200k load applications	After 2.67 M load applications
asphalt concrete / ATPB	5.5	16.4	NA	NA
ATPB / aggregate base	NA	NA	23.6	23.0
aggregate base	23.7	19.1	NA	NA
aggregate subbase	6.6	10.4	13.9	14.7
subgrade	64.2	54.1	62.5	62.3

NA MDD modules were not placed at these locations (see Figure 2.2)
Note: Calculated from Table 3.10

3.5 VISUAL INSPECTIONS

Crack monitoring is an essential part of data collection since it is used to measure surface cracks which are the physical manifestation of fatigue distress in asphalt pavements. The monitoring procedure included visual inspections of the test pavement, direct measurement of the crack length, photographic documentation of the surface cracks, and graphical representation of cracking progress. The Optimas® software package was used to analyze the cracking in asphalt pavement as described in Section 3.5.2.

This section discusses the extent and severity of surface cracking and details the methodology used to obtain this information with a description of the digital image analysis procedure used for the first time with Section 501RF. The crack data begins at 1.3 million repetitions when cracks were first observed, and covers 90 cm of the 1 meter width and the

6 meters along the length of the test section from Point 2 to Point 14 (to avoid the turnaround areas between Points 0 and 2, and Points 14 and 16).

3.5.1 Visual Inspection of Cracks

The first surface cracks were observed at approximately 1.3 million repetitions and regular inspection of crack development was made from then on to the end of the test. To obtain crack length data, the pavement was illuminated with high-power lights followed by the marking of the cracks with lumber crayon in order to make them easily visible and photographable. A small chain was then laid out on each crack along its course and then stretched out and measured with a ruler. The observed average crack length obtained by this method as a function of load repetitions is shown in Figure 3.21.

It should be noted that operator error is possible with this method of crack detection. Such error was particularly evident for the data reported for Section 500RF *(3)*, which displayed a high degree of fluctuation in the total measured crack length. As with Section 500RF, the observed cracks in this section were hairline cracks and at times difficult to detect visually. Operator error is presumed to result in fewer cracks being detected than actually exist. The influence of operator error is greatly diminished with the implementation

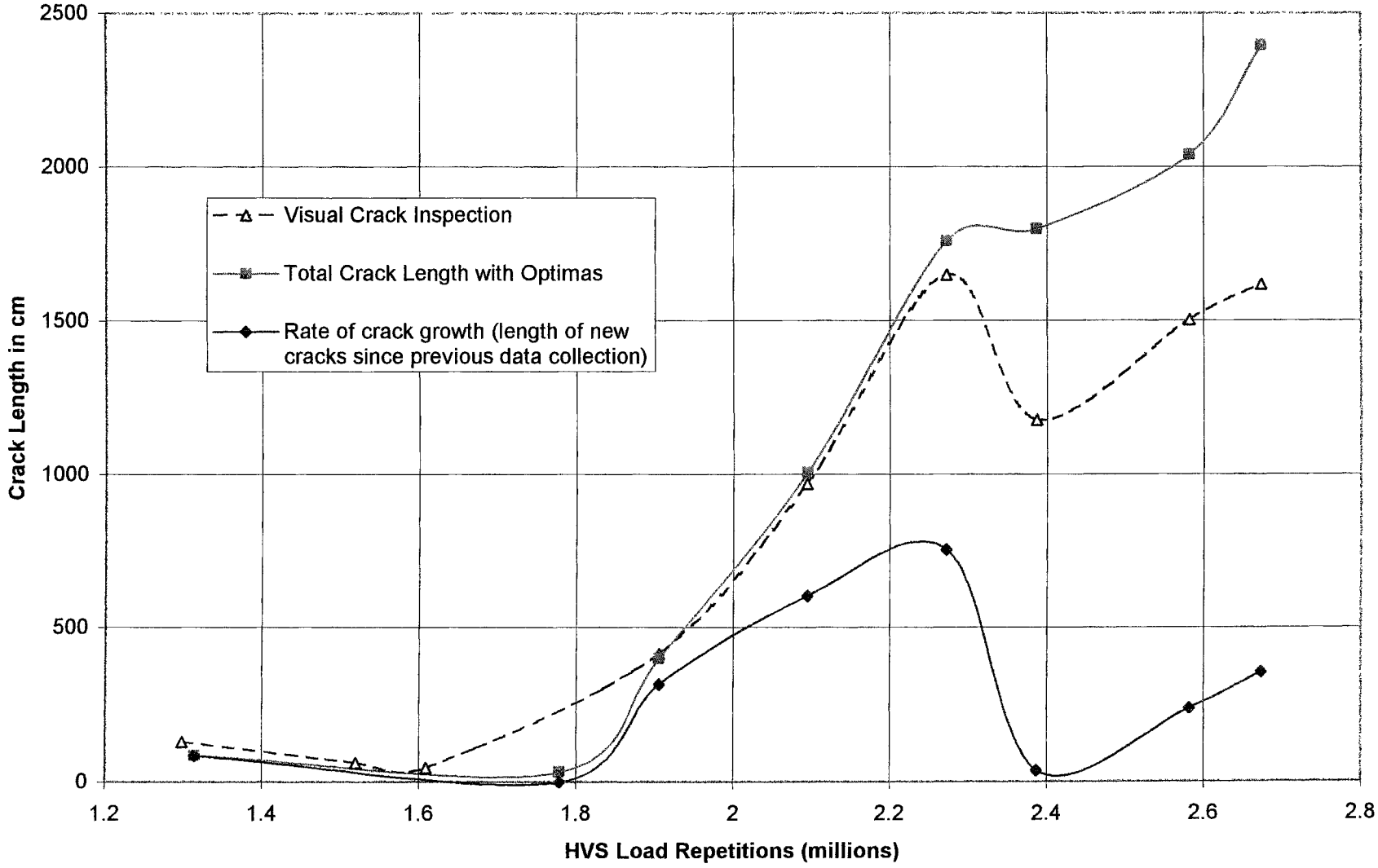

Figure 3.21 Crack length development for Section 502CT

of a digital method of crack observation and analysis method described in detail in the following Section 3.5.2.

The lack of expansion, spalling, and other deterioration of the hairline cracks observed on the pavement surface can likely be attributed to two factors:

- lack of rainfall and mineral particles on the surface of the test pavement, and
- lack of cracking in the lower lift of asphalt concrete.

These factors were both discussed at length in the 500RF report *(3)*.

3.5.2 Digital Analysis of Cracks

Figures 3.22 through 3.27 show crack length as determined by digital image analysis at crack initiation (1.31 million repetitions) and five other times during crack propagation, at 1.78, 1.91, 2.27, 2.37, and 2.67 million repetitions. The process for digitally analyzing crack length was developed during testing of Section 501RF, weeks before crack initiation occurred on Section 502CT. A variety of quantitative information is available from images of cracks through digital image analysis. The Optimas® software employed is a package available from Optimas® Corporation. A description of the process follows.

The test section is marked with a lumber crayon as with visual inspection, and then photographed in sections with a medium-format (60 mm×70 mm) camera. The photographs are then digitized, adjusted to remove camera perspective and distortion, and then recombined to create a composite 2-dimensional image of the test section. The cracks from this composite image are then traced in Optimas® and the image is then calibrated to the real-life dimensions of the test section, as seen in Figures 3.22 through 3.27. Crack statistics can then be calculated and further analyses performed on the crack data.

The first real advantage of this method is the elimination of some operator error. In the Section 500RF report *(3)*, the plot showing total crack length on the test section displayed a great deal of fluctuation due to operator error in detecting cracks. With the digital method, starting with the first crack photos, an overlay is created from the traced cracks. This overlay is then placed over the next set of crack photos. Then, when the crack image of the second set is traced, cracks which appear to have decreased in length, or with portions missing or undetected by the technicians performing crack monitoring, can be traced via the overlay along with the new cracks which were detected. The crack trace from this image is then used as an overlay for the next set of crack photos creating a cumulative assessment of crack progress. This process is then repeated through all the sets of crack photos until the end of the test.

This method may raise suspicion over the possibility of "healing." It was found, however, that all the cracks which may have "disappeared" and "reappeared" later, or which shortened and then lengthened again, were doing so in the exact same location and would, without exception, progress over the duration of the test though they may have been undetected during some crack inspections. Verification of this phenomenon, which seems to be a function of accelerated pavement testing, is only possible through the use of digital techniques. Moreover, the overlays matched successive crack photos exactly. On occasion, camera perspective could cause some uncorrectable distortion which would offset the overlays slightly. However, this offset was never more than 2 cm in the calibrated image, an error of 0.25 percent.

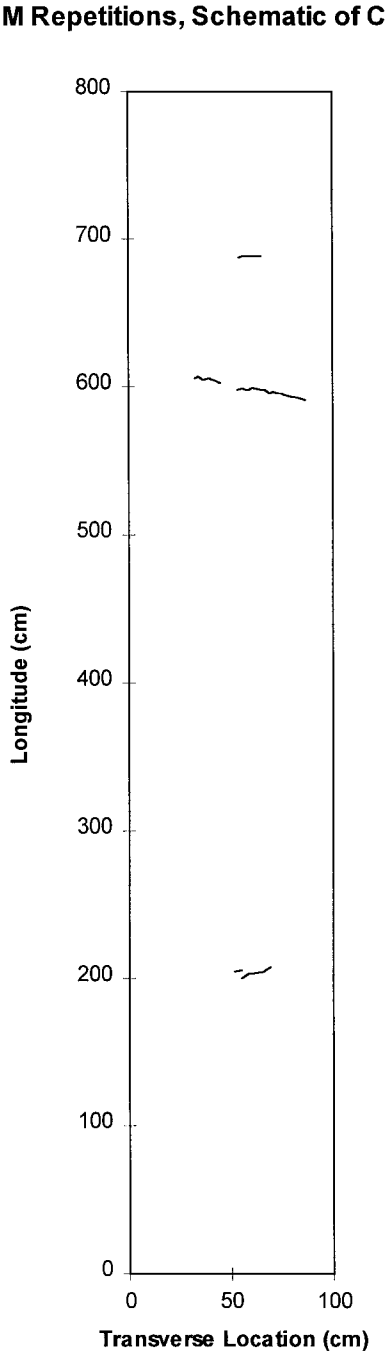

Figure 3.22 Optimas® cracks at 1.31 million repetitions

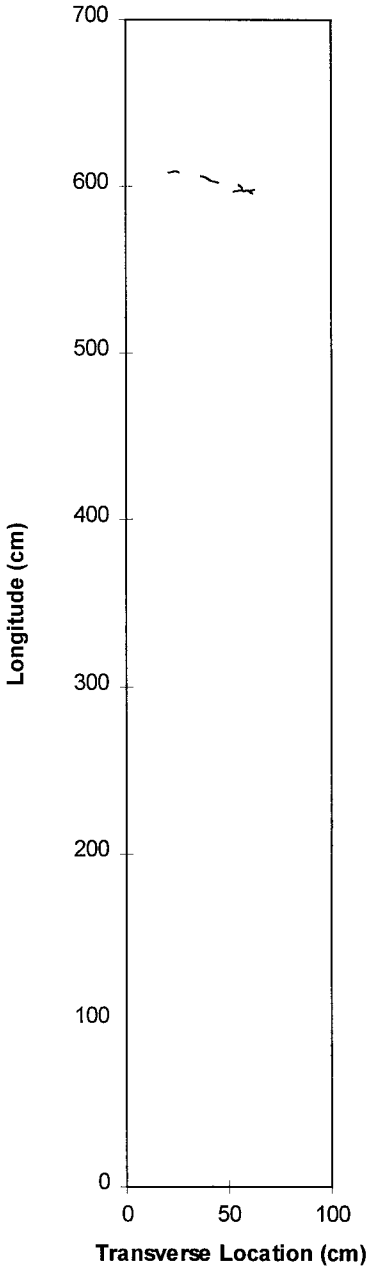

Figure 3.23 Optimas® cracks at 1.78 million repetitions

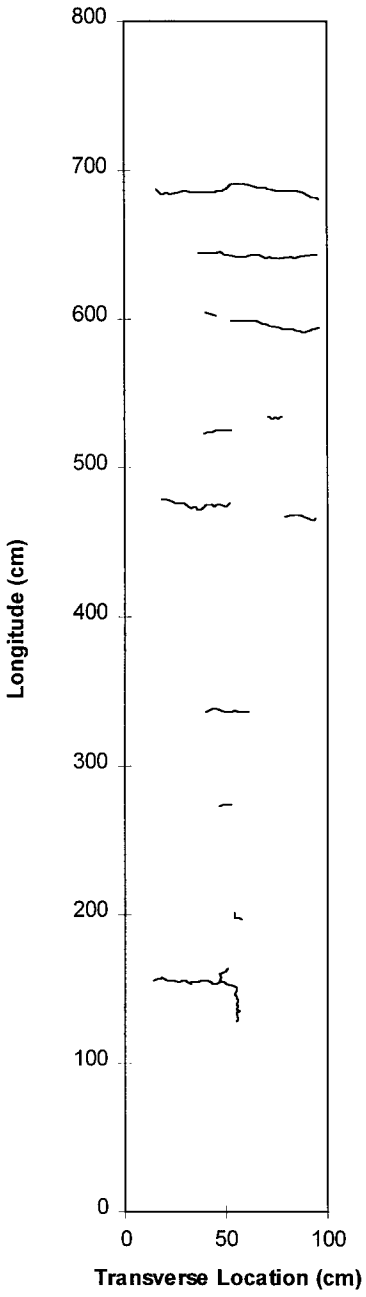

Figure 3.24 Optimas® cracks at 1.91 million repetitions

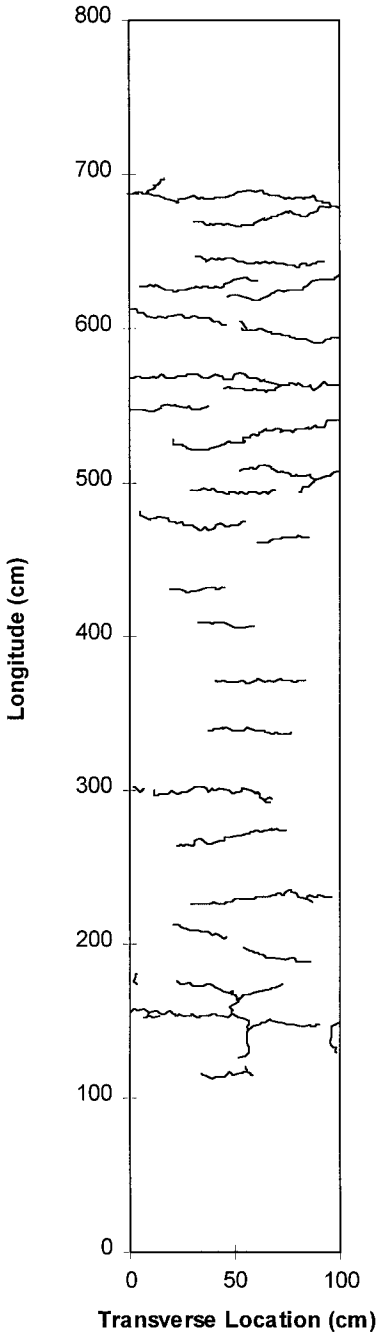

Figure 3.25 Optimas® cracks at 2.27 million repetitions

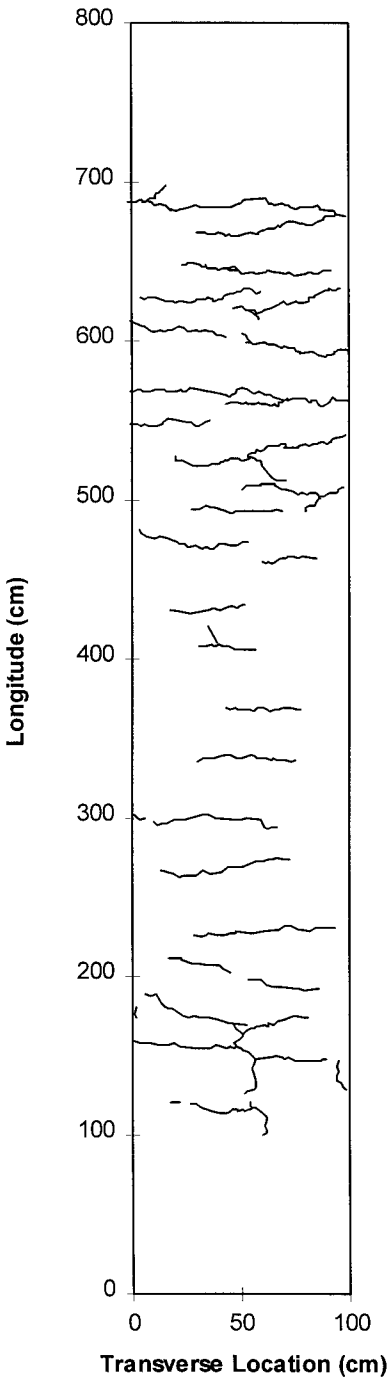

Figure 3.26 Optimas® cracks at 2.37 million repetitions

502CT, 2.67M Repetitions, Schematic of Cracking Pattern

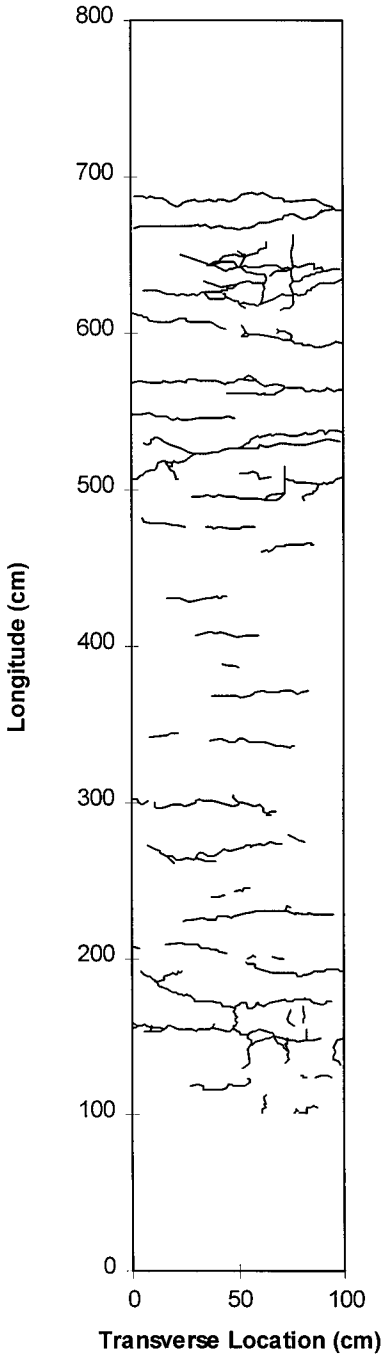

Figure 3.27 Optimas® cracks at 2.67 million repetitions

3.5.3 Assessment of Cracking on Section 501RF

Figure 3.26 shows that the pavement cracked much like Section 500RF. Soon after cracks were first detected at approximately 1.31 million repetitions, a period of rapid crack growth ensued from 1.8 million to 2.3 million repetitions. Crack growth ceased for 200,000 repetitions between 2.3 and 2.5 million repetitions, but then resumed for the remainder of the test. Had the test been run longer, it can be assumed that the crack pattern would resemble extensive alligator cracking, where the pavement behaves as a series of individual blocks, or "cobbles," separated by cracks. A look at the final crack diagram in Figure 3.27 shows the extent of cracking experienced on Section 502CT; at this point the surface is fairly well cracked, exemplifying "alligator cracking" at Points 3 and 13 (longitudinal Stations 150 and 650 cm).

Figures 3.22 to 3.27 provide a digital picture of the cracking exactly as it occurred in the pavement. The effect of the wandering load is evident, as cracking is focused along the centerline of the test section, as would be expected given the loading pattern of the HVS test wheel. In addition, these figures show longitudinal differences. Specifically, the high degree of cracking that occurred between Points 10 and 14 and Points 2 and 4, and the negligible amount of cracking which occurred between Points 6 and 10. The crack data correlated with RSD, MDD, and profilometer data is discussed in Section 3.4. It can be seen from Figures 3.19 and 3.20 that the largest RSD deflections were consistently measured at Point 12, where the most cracking occurred. Figures 3.17a and 3.17b indicate that deflections along the centerline are greater than at the lateral offsets, which matches the cracking pattern and the HVS lateral wander pattern.

3.5.4 Cracks in Cores Taken from Section 502CT

In the Interim Report *(2)* it had been noted, from inspection of some cores taken after construction for mix evaluation, that there appeared to be little or no bond between the two asphalt concrete lifts. No tack coat was placed between the lifts because it was not required by Caltrans specifications, and would not have been used in typical Caltrans practice. However, a tack coat would likely have contributed to an improved bond between the lifts. The four cores taken from within or near Section 502CT also showed no bonding between lifts and cracking only in the upper asphalt concrete lift, and not in the lower asphalt concrete lift.

As will be shown in Chapter 4, the absence of a tack coat and resultant weak bond between the two asphalt concrete lifts resulted in the critical horizontal tensile strain occurring at the bottom of the top asphalt concrete lift. As a result, crack formation started in this location rather than on the underside of the lower asphalt concrete layer.

CHAPTER 4

SECTION 502CT PERFORMANCE EVALUATION

When the accelerated pavement testing using the Heavy Vehicle Simulator (HVS) was completed, Section 502CT had been subjected to 150,000 applications of 40-kN loading, 50,000 applications of 80 kN loading, and 2,470,000 applications of 100-kN loading. According to the Caltrans procedure[5], Section 502CT experienced approximately 117,000,000 equivalent single axle loads (ESALs) during its useful life, significantly greater than its design life of approximately 1,000,000 ESALs. The primary purpose of this chapter is to investigate this difference between the predicted Caltrans design loading and the performance of the test section.

As stated in Reference *(3)*, the Caltrans flexible pavement design procedure does not identify nor distinguish among various modes of pavement distress and does not enable detailed examination of many of the factors that can affect pavement performance. As a result, the methodology described in Reference *(3)* for Section 500RF will be used to analyze Section 502CT since the predominant distress mode was surface cracking due to fatigue. This surface cracking was visible throughout the test section, averaging 4.0 m in length for each square meter of area.

Some surface rutting was also observed, with an average rut depth at the surface of 9.8 mm. MDD measurements indicated that the asphalt-bound layers (asphalt concrete and asphalt treated permeable base) contributed approximately 60 percent to this average followed by 16 percent for the aggregate base, 11.5 percent for the subbase, and 12.5 percent for the

---

[5] Load equivalency factor = (wheel load in kN/40)$^{4.2}$.

subgrade (Table 3.6). The influence of the untreated materials on performance based on the Asphalt Institute's subgrade strain criteria *(11)* is also included.

4.1 FATIGUE ANALYSIS AND DESIGN SYSTEM

The fatigue analysis and design system used herein is the same as that used to analyze the other test sections; the framework for this system is illustrated in Figure 4.1. It considers not only fundamental mix properties but also the level of design traffic, the temperature environment at the site, the pavement structural section, laboratory testing and construction variabilities, and the acceptable level of risk.

4.1.1 System Description

The system shown in Figure 4.1 is used herein to estimate the number of ESALs that can be sustained either in a design setting or in the HVS enclosure at the Richmond Field Station. The parameters used to determine ESALs have already been described *(12)*. The critical strain, determined using CIRCLY *(13)*, permitted determination of the shift factor, SF, according to the equation (Figure 4.1).

$$SF = 3.1833 \times 10^{-5} \varepsilon^{-1.3579}$$

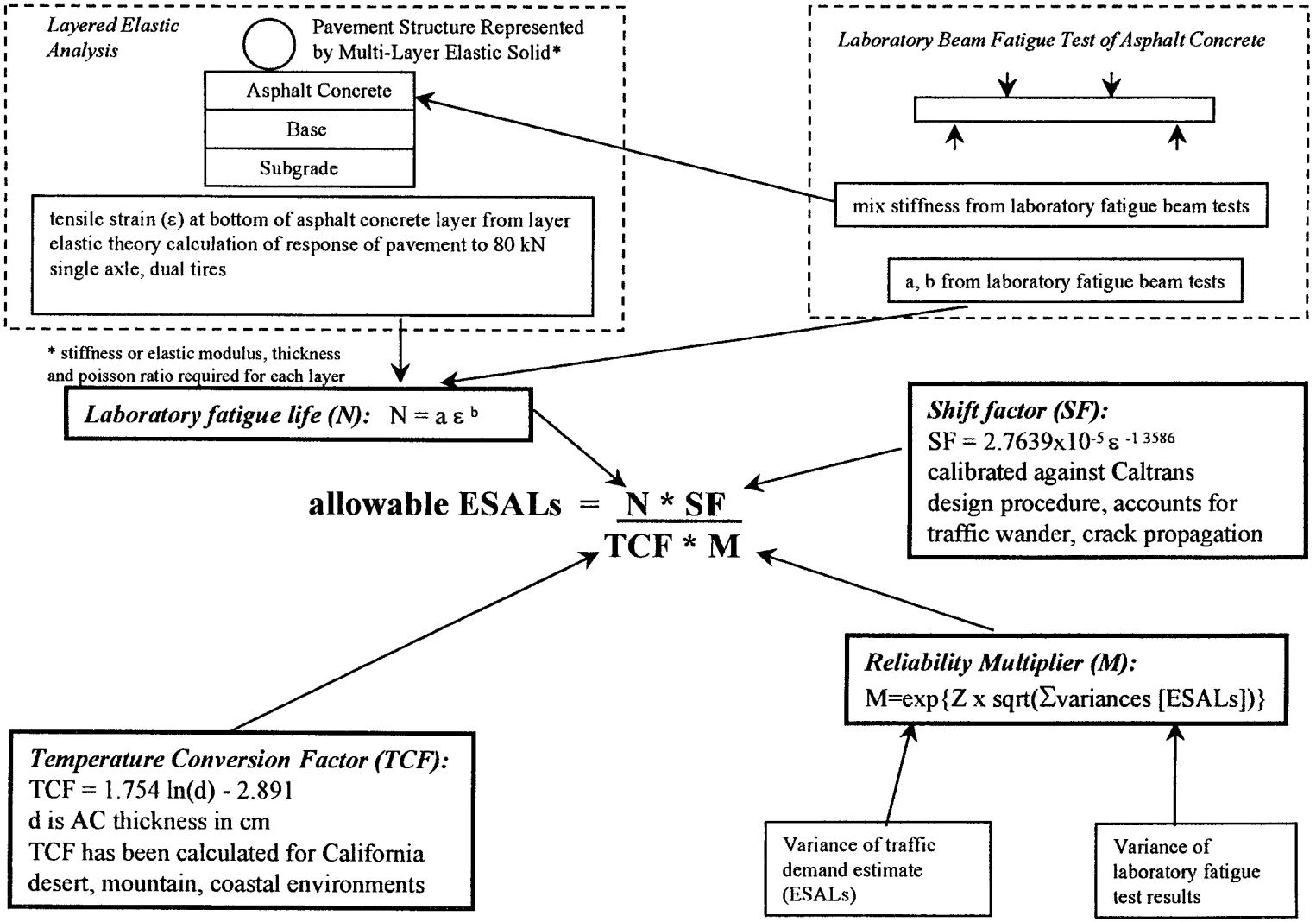

Figure 4.1 Methodology followed in the fatigue analysis system to determine ESALs

The temperature conversion factor, TCF, used for in-situ performance simulations is that derived earlier for a coastal environment *(12)* (Figure 4.1):

$$TCF = 1.754\ln(d) - 2891$$

The reliability multiplier, M, is determined from the expression (Figure 4.1):

$$M * e^{z\sqrt{var(lnN) * var(lnESALs)}}$$

The factor Z varies from 0 at a design reliability of 50 percent to 2.05 at a design reliability of 98 percent *(14)*.

Variance in the logarithm of the laboratory fatigue life, var(ln N), has been calculated using a Monte Carlo simulation procedure. This procedure accounts for the inherent variability in fatigue measurements; the nature of the laboratory testing program (principally the number of test specimens and the strain levels); the extent of extrapolation necessary for estimating fatigue life at the design, in-situ strain level; mix variability due to construction (namely asphalt and air-void contents); structural variability due to construction (namely thickness of the asphalt concrete surface and the equivalent stiffness or modulus of supporting layers). Variances for these parameters considered representative of prevailing California construction practice have been used herein *(15)*. Variance associated with uncertainty in the traffic estimate, var(ln ESALs) of 0.3, has also been used in the calculations.

4.1.2 Important Differences Between Pavement Design and HVS Testing

Summarized in this section are some of the factors that help to explain the difference between the Caltrans design estimate of approximately 1,000,000 ESALs and the HVS measurement of approximately 117,000,000 ESALs. Recognized and emphasized at the outset is the unknown error that results from assuming that the Caltrans design estimate is dictated primarily by the prevention of premature fatigue cracking and not other distress modes.

One fundamental difference between a pavement design estimate and the corresponding test measurement is that the design must accommodate a range of mixes of varying performance characteristics and must incorporate a safety factor to prevent premature failure as a result of testing, construction, and traffic variability. A direct measurement in the HVS test, on the other hand, reflects the performance characteristics of a specific mix, it is independent of laboratory testing and traffic variability; and, because the test section is limited to a relatively small area, 1 m. $\times$ 8 m. in plan, the influence of construction variability is minimal. The design estimate is always expected to be much smaller in magnitude than the test measurement with the difference between the two increasing as the design reliability increases. The fatigue design and analysis system used herein has the ability to distinguish between design estimates and test measurements and to assess the impact of reliability on design estimates. No reliability factor is associated with simulations of HVS test ESALs for the reasons described above.

Another difference between design and testing relates primarily to pavement structural effects. In the current case, four notable differences distinguished Section 502CT from its design scenario including a top asphalt concrete lift thickness of 68 mm instead of 61 mm, a lower asphalt concrete lift thickness of 80 mm instead of 76 mm, a thickness of subbase of 215 mm instead of 229 mm, a difference in the air void contents within the two asphalt

concrete lifts instead of uniform air voids, and a largely unbonded interface between the lifts instead of a fully bonded one *(2)*.

Important differences are also found between the standard mix used for calibrating the fatigue analysis and design system and that used in HVS Section 502CT. Asphalt and air-void contents for the standard mix were set at 5 and 8 percent, respectively, representing the approximate asphalt content found from the Caltrans mix design procedure and relative compaction of about 97.3 percent. The asphalt content for the mix used in Section 502CT averaged 4.8 percent, also based on the Caltrans procedure. Air-void contents averaged 7.6 percent in the upper lift and 4.0 percent in the lower lift corresponding to about 96.3 percent and 100.0 percent relative compaction respectively for mix.

In addition to differences in degree of compaction, there were other differences between the standard mix and the mix used in the HVS test section. That is:

1. aggregates for the two mixes came from different sources and did not have the exactly same gradations, although both as-constructed gradations met Caltrans's standard specifications for 19-mm coarse Type A mixes;
2. asphalt binders in both mixes were identified as being from California Valley sources and exhibited similar rheological and aging behavior in laboratory tests performed at the Caltrans ESC, Sacramento *(16)*. The binders were, however, produced about 6 years apart and not necessarily at the same refinery nor using the same processes; and
3. laboratory test results for the mix from the HVS test were obtained from beams cut from the test pavement soon after construction, while laboratory

test results for the standard mix were obtained from laboratory mixed and compacted specimens.

In all likelihood, however, specimen compaction is not a source of the differences; comparison of laboratory test results on beams sawed from the test pavement and obtained by laboratory rolling wheel compaction exhibited little difference in stiffness and fatigue properties *(2)*. Moreover large differences in mix properties caused by laboratory mixing and short-term oven aging (STOA) versus plant mixing are also considered unlikely at this time although they have only been evaluated in terms of mix and binder stiffness and not in terms of fatigue properties. More data will be obtained from future CAL/APT test pavements to compare differences in fatigue properties between laboratory mixed and plant–mixed, laboratory compacted specimens.

As reported elsewhere *(11)*, laboratory testing of the standard mix yielded the following expressions:

$$\ln N = -22.0012 - 0.164566AV + 0.575199AC - 3.71763 \ln \varepsilon$$

and

$$\ln S = 10.282 - 0.076AV - 0.172AC$$

where N = laboratory fatigue life in a third-point loading controlled-strain flexural test,

AV = air-void content in percent,

AC = asphalt content in percent,

ε = flexural strain, and

S = laboratory flexural stiffness in MPa.

For the HVS mix *(2)*, the following expressions were obtained at the 4.8 percent asphalt content:

$$\ln N = -21.9252 - 0.106663AV - 4.14248 \ln \varepsilon$$

and

$$\ln S = 9.5603 - 0.084914AV$$

where S is again expressed in MPa.

Based on these results, the laboratory determined fatigue life of the HVS mix is two to eight times that of the standard mix, depending on strain level, while its stiffness is only 1 to 8 percent larger. Thus, the HVS mix is expected to exhibit improved performance over the standard mix.

These results emphasize the importance of laboratory fatigue testing to assess fatigue performance to insure a realistic estimate of pavement performance and in particular, in insuring proper interpretation of the HVS test results.

Environmental differences also distinguish the HVS test conditions from specific field pavement sites. These include the effects of temperature and moisture differences.

In the 500RF report *(3)*, for example, it was demonstrated that during the period of that test (May to November), the temperature environment of the HVS was slightly more severe than the coastal environment, i.e. the predicted ESALs for the HVS site were about 85 percent of the number that could be sustained in situ.

The second major environmental difference is due to the effects of moisture. The protected HVS environment limits the amount of moisture in the pavement and practically eliminates cyclic wetting and drying. The net effect is expected to be beneficial. Moisture effects are simulated in this analysis by assuming that effective moduli of all supporting layers

(aggregate base, aggregate subbase, and subgrade) under natural conditions are 80 percent of those in Section 502CT. It must be emphasized that the 80 percent is an assumed quantity used for illustration purposes only. It is not a result of detailed scientific inquiry.

Quantification of the effects of these differences, using the fatigue analysis and design system, is the objective of the next section.

4.1.3 General Performance Analysis

For this analysis, the computer code, CIRCLY, was used to compute critical strain levels. The applied load consisted of a 40-kN (9,000-lb) wheel load distributed on dual tires (305 mm [12.0 inches] center-to-center) with a contact pressure of 690 kPa (100 psi). A distinction was made between Section 502CT *design conditions* and the as-built and as-tested *HVS conditions* with respect to layer thicknesses and environmental influences. Quantitatively the differences are as follows in Table 4.1.

Table 4.1 Comparison of Section 502CT design conditions and HVS conditions

	Design conditions	**HVS conditions**
Thickness of upper asphalt concrete lift (mm)	61	68
Thickness of aggregate subbase (mm)	229	215
Moduli of supporting layers (MPa) Aggregate Base Aggregate Subbase Subgrade	240 120 56	300 150 70

Further distinction was made between a *standard mix* and the *HVS mix*. The standard mix was that used in calibrating the fatigue analysis and design system. Components included a Watsonville granite and an AR-4000, apparently from California valley sources. Asphalt and air-void contents were assumed to be 5 and 8 percent respectively. The HVS test utilized a different aggregate but the grading was similar to that of the standard mix; both gradings

conformed to the Caltrans specifications for the Type A, 19-mm-maximum size, coarse gradation. The asphalt was an AR-4000 from California Valley sources, and the asphalt content of the mix was 4.8 percent. Air voids averaged 7.6 percent in the upper lift and 4.0 percent in the lower lift.

The temperature environment was essentially ignored for the General Performance Analysis, with a constant temperature of 20°C assumed for both design conditions and HVS conditions. This assumption results in a TCF of 1.00 because the laboratory test temperature is 20°C.

Five different cases, defined as follows, were analyzed as shown in Table 4.2:

Table 4.2 Definition of five cases

Case	Description	Critical strain location
1	Design conditions with standard mix (8% air void content and 5% asphalt content); full friction interface	Bottom of lower lift
2	HVS conditions with standard mix (8% air void content and 5% asphalt content); full friction interface	Bottom of lower lift
3	HVS conditions with standard mix (4.0% air void content bottom lift, 7.6% air void content top lift and 5% asphalt content); full friction interface	Bottom of lower lift
4	HVS conditions with HVS mix (4.0% air void content bottom lift, 7.6% air void content top lift and 4.8% asphalt content); full friction interface	Bottom of lower lift
5	HVS conditions with HVS mix (4.0% air void content bottom lift, 7.6% air void content top lift and 4.8% asphalt content); frictionless interface	Bottom of upper lift

Elastic parameters used in the CIRCLY computations are identified in Table 4.3.

Table 4.3 Elastic parameters for CIRCLY analyses

Layer	Case				
	1	**2**	**3**	**4**	**5**
Modulus (MPa)					
Upper Asphalt	6,736	6,736	6,943	7,442	7,442
Lower Asphalt Concrete lift	6,736	6,736	9,121	10,104	10,104
Asphalt Treated Permeable Base	827	1,034	1,034	1,034	1,034
Aggregate Base	240	300	300	300	300
Aggregate Subbase	120	150	150	150	150
Subgrade	56	70	70	70	70
Poisson's ratio					
Upper Asphalt Concrete lift	0.35	0.35	0.35	0.35	0.35
Lower Asphalt Concrete lift	0.35	0.35	0.35	0.35	0.35
Asphalt Treated Permeable Base	0.4	0.4	0.4	0.4	0.4
Aggregate Base	0.35	0.35	0.35	0.35	0.35
Aggregate Subbase	0.35	0.35	0.35	0.35	0.35
Subgrade	0.45	0.45	0.45	0.45	0.45
Thickness (mm)					
Upper Asphalt Concrete lift	61	68	68	68	68
Lower Asphalt Concrete lift	76	80	80	80	80
Asphalt Treated Permeable Base	76	76	76	76	76
Aggregate Base	182	182	182	182	182
Aggregate Subbase	229	215	215	215	215
Subgrade	Semi-infinite	Semi-infinite	Semi-infinite	Semi-infinite	Semi-infinite

These represent the best estimates of the stiffnesses of the pavement components based on laboratory determined and in-situ measured response characteristics, the latter having been computed from FWD measurements *(2)*.

The first matter to be addressed includes both the effect of reliability on estimates of design ESALs as well as the fundamental difference between design ESALs [whether from the Caltrans or UCB-ISAP procedures *(15)*],and HVS ESALs (whether measured under HVS loading or simulated using the UCB-ISAP system). In computing HVS ESALs, variances of the several parameters (asphalt content, air-void content, asphalt concrete thickness, foundation support, and traffic) were assumed to be negligible. Computations using the UCB-ISAP system for Case 1 conditions yield the following ESAL estimates (Table 4.4):

Table 4.4 Simulated HVS ESALs for Case 1

Simulated HVS ESALs	**UCB-ISAP Design ESALs for reliability of:**			
	80%	90%	95%	98%
8,175,000	3,443,000	2,193,000	1,514,000	994,000

This table shows the influence of reliability on design ESALs, the 8,175,000 simulated HVS ESALs is considerably greater than any of the design ESALs: for a design reliability level of 90 percent, the computed ratio of simulated HVS ESALs to UCB-ISAP design ESALs is approximately 3.7.

The 90 percent design reliability estimate, assuming a constant 20°C asphalt concrete temperature and no water damage to the ATPB, is 2,193,000 ESALs, greater than the Caltrans design estimate of 1,000,000 ESALs. The UCB-ISAP fatigue analysis and design system estimate of 994,000 ESALs at 98 percent reliability is nearly the same as the Caltrans design

estimate, again assuming a 20°C asphalt concrete temperature and no damage to the ATPB water. An analysis of the effect of pavement temperature for the California Coastal environment is presented later in this chapter.

Next, in order to demonstrate the significant difference between as-built and as-tested HVS conditions and the assumed Caltrans design conditions, the simulated HVS ESALs estimate for Case 2 was compared with that for Case 1 with the results shown in Table 4.5:

Table 4.5 Comparison of simulated HVS ESALs—Case 1 to Case 2

Simulated HVS ESALs for:	
Case 1	**Case 2**
Design conditions with standard mix (8% air void content and 5% asphalt content): full friction interface	HVS conditions with standard mix (8% air void content and 5% asphalt content): full friction interface
8,175,000	23,397,000

The ratio of HVS ESALs for HVS conditions to that for design conditions is approximately 2.9. The enhanced simulated performance for the HVS environment stems from a combination of thickness differences and the assumed effect of moisture.

To demonstrate the effect of the excellent mix compaction achieved in the construction of Section 502CT, particularly of the lower lift, the simulated HVS ESALs estimate for Case 3 was compared with that for Case 2, Table 4.6:

Table 4.6 Comparison of simulated HVS ESALs—Case 2 to Case 3

Simulated HVS ESALs for:	
Case 2	**Case 3**
HVS conditions with standard mix (8% air void content and 5% asphalt content): full friction interface	HVS conditions with standard mix (3.2% air void content bottom lift, 7.2% air void content top lift and 5% asphalt content): full friction interface
23,397,000	96,244,000

The very significant effect of air-void content is illustrated by a ratio of approximately 4.1 in the HVS ESALs estimate for a 4.0 percent bottom lift and 7.6 percent top lift compared to that for an 8-percent mix in both lifts. This finding emphasizes the importance of good construction practice and the potential impact of improved compaction above that required in current Caltrans specifications typically require. An even larger improvement in simulated fatigue life than that shown here would have been observed if the 4.0 percent air-void content had been obtained in both lifts. These corroborate similar findings for a variety of typical Caltrans pavement structures reported previously *(12)*.

To demonstrate the effect of the superior fatigue performance of the HVS mix compared to the standard mix, the simulated HVS ESALs estimate for Case 4 was compared with that for Case 3. Results are in Table 4.7:

Table 4.7 Comparison of simulated HVS ESALs—Case 3 to Case 4

Simulated HVS ESALs for:	
Case 3	**Case 4**
HVS conditions with standard mix (4.0% air void content bottom lift, 7.6% air void content top lift and 5% asphalt content): full friction interface	HVS conditions with HVS mix (4.0.% air void content bottom lift, 7.6% air void content top lift and 4.8% asphalt content): full friction interface
96,244,000	487,314,000

The ratio of Simulated HVS ESALs for these two conditions is approximately 5.1. This large difference is not clearly attributable to any one particular component of the two mixes, and is

likely due to a combination of potential differences in components including asphalt production and aggregate type and gradation.

It should be noted that the Simulated HVS ESALs for Case 4 (487,314,000) exceeds the measured number of 117,000,000 HVS ESALs (assuming a 4.2 exponent for load equivalency). A part of this difference may well be due to imprecision of the fatigue analysis and design system, to inappropriate assumptions made for this analysis, and/or to important factors not yet identified and accounted for.

One such factor relates to the lack of bonding at the interface between upper and lower asphalt concrete lifts. CIRCLY allows an examination of the interface condition but, unfortunately, only at the two extremes, full-friction and frictionless interfaces. The interface condition of Section 502CT is likely somewhere between these two extremes: the interface is rough and the weight of the upper layer combined with vertical compressive stress beneath the load should allow some transfer of stress across the surface. Even though partial friction conditions can not be modeled with techniques used in this analysis, the notable effect of interface condition can be demonstrated by comparing the HVS ESALs estimate for Case 5 with that for Case 4. Results are shown in Table 4.8:

Table 4.8 Comparison of simulated HVS ESALs—Case 4 to Case 5

Simulated HVS ESALs for:	
Case 4	**Case 5**
HVS conditions with HVS mix (3.2% air void content bottom lift, 7.2% air void content top lift, and 4.8% asphalt content): full friction interface	HVS conditions with HVS mix (3.2% air void content bottom lift, 7.2% air void content top lift, and 4.8% asphalt content): frictionless interface
487,314,000	17,963,000

This remarkably large effect is due to two factors, one of which is the nature of friction at the interface between lifts. The other results from a shift in the critical strain location from the bottom of the lower lift for the full friction interface to the bottom of the upper lift for the frictionless interface. In the upper lift, the air-void content is greater and load repetitions necessary to propagate cracks to the top surface are expected to be smaller because of the reduced thickness through which the cracks must penetrate. The combined effect of a larger air-voids content and a reduced overlying thickness results in a significant decrease in simulated fatigue life.

Although this analysis is not definitive because the interface condition cannot be accurately modeled, the measurement of 117,000,000 ESALs under HVS loading falls between the estimates of 17,963,000 for the frictionless case and 487,314,000 for the full friction case, which follows the qualitative evaluation of interface conditions discussed in Chapter 3. The simulation results indicating that cracking would occur in the upper lift before it occurred in the lower lift for the frictionless interface condition corroborate the cracking observations from Section 502CT cores. Certainly the analysis reported herein is of significant help in reconciling the difference between the Caltrans design estimate of 1,000,000 ESALs and the HVS test measurement of 117,000,000 ESALs. In addition the analysis has highlighted factors such as

mix, air-void content and interface condition that can have a significant impact on pavement performance.

4.1.4 Estimate of Design ESALs for California Coastal Environment

In Reference *(3)*—the 500RF report—pavement performance in the HVS test was observed during the period May to November 1995. By comparing the performance with that for comparable periods of time in three regions of California for which Temperature Conversion Factors (TCF) had been determined *(12)*, it was demonstrated that the test conducted at the HVS site was more damaging than for comparable traffic conditions at the three in-service sites.

As with the analyses in the 501RF and 503RF, it was decided to examine an alternative approach and compare, across the entire year, the performance of the pavement at a constant temperature of 20°C at the HVS site with the variable temperature regime for the California Coastal environment. For Case 1 of the General Performance Analysis (standard mix, design conditions, 8 percent air-voids content, 5 percent asphalt content), the TCF computed for the California Coastal environment is 1.702. Assuming that the mix used to develop temperature conversion factors has a temperature susceptibility similar to that of the standard mix, application of this TCF to Case 1 of the General Performance Analysis results in the estimates shown in Table 4.9.

Table 4.9 Estimates of design ESALs applying the TCF for the Coastal environment to Case 1

Simulated HVS ESALs	UCB-ISAP Design ESALs for reliabilities of:			
	80%	90%	95%	98%
4,803,000	2,023,000	1,288,000	889,500	584,000

For this assumption, it can be seen that the estimated fatigue life for 90 percent reliability is slightly more than the Caltrans design estimate of 1,000,000 ESALs. It should be noted, however, that this number of ESALs represents the middle of the range in traffic (800,000–1,270,000 ESALs) corresponding to a Traffic Index (TI) of 9, the traffic parameter for the structural section design. Thus at a reliability level of 90 percent, it could be concluded that the design is adequate within the bounds of traffic associated with a TI of 9.

4.2 SUBGRADE DEFORMATION

The Caltrans pavement design procedure is intended to prevent premature failure from rutting as well as from fatigue cracking. At the termination of HVS trafficking, the average rut depth at the surface of Section 502CT was approximately 9.8 mm. This is less than the limiting rut depth of 13 mm (0.5 in.) stipulated by Caltrans as a part of its performance requirements. MDD measurements indicated that about 40 percent of the permanent deformation was contributed by the aggregate base, subbase, and subgrade.

A comprehensive procedure for evaluating the potential for rutting in the underlying layers including reliability (like that for fatigue) has not been developed as yet. An evaluation of the Section 502CT pavement with respect to rutting resulting from deformations in the untreated layers was performed using the Asphalt Institute criteria for vertical compressive strain at the top of the subgrade. This analysis was performed for the same five cases used for the fatigue evaluation.

4.2.1 Subgrade Rutting Criteria

The Asphalt Institute criteria for vertical compressive strain are obtained from the expression:

$$N = 1.05 * 10^{-9} \varepsilon_c^{-4.484}$$

where N = number of load applications, and

ε_c = vertical compressive strain at subgrade surface.

The equation was first incorporated in a pavement design procedure by Santucci and is based on analyses of pavements designed according to the Caltrans design procedure *(17)*. The authors of the Asphalt Institute methodology using this subgrade stain relation state, *"if good compaction of the pavement components is obtained and the asphalt mix is well designed, rutting should not exceed about 13 mm (0.5 in.) at the surface for the design traffic, N."* This statement implies some conservatism in the criteria; however it does not include an explicit factor of safety or reliability estimate.

The vertical compressive strain at the top of the subgrade was calculated using the program CIRCLY, for the 40-kN (9,000-lb) dual tire wheel load (305-mm [12.0-in.] center-to-center) and 690-kPa (100-psi) contact pressure, and the pavement structures shown earlier. The difference in thermal environment between the design conditions and HVS conditions was not addressed in this study. The asphalt concrete stiffness utilized for the subgrade strain computations is that at 20°C, approximately the temperature maintained at the surface of the Section 502CT pavement. A temperature sensitivity study of the type used to estimate the effects on fatigue life of in-situ temperatures for typical California environments has not been performed for subgrade rutting.

4.2.2 Subgrade Rutting Performance Analysis

The permissible ESALs for the calculated subgrade strain for each of the five cases are compared with the simulated HVS ESALs to fatigue failure in Table 4.10.

Table 4.10 Comparison of permissible ESALs for subgrade strain to simulate HVS ESALs to fatigue failure for five cases

Case	Permissible ESALs by Asphalt Institute Subgrade Strain Criteria	Simulated HVS ESALs to Fatigue Failure
Design conditions with standard mix (8% air void content and 5% asphalt content), full friction interface (Case 1)	18,735,000	8,175,000
HVS conditions with standard mix (8% air void content and 5% asphalt content), full friction interface (Case 2)	48,163,000	23,397,000
HVS conditions with standard mix (3.2% air void content bottom lift, 7.2% air void content top lift and 5% asphalt content), full friction interface (Case 3)	55,531,000	96,244,000
HVS conditions with HVS mix (3.2% air void content bottom lift, 7.2% air void content top lift and 5% asphalt content), full friction interface (Case 4)	61,217,000	487,314,000
HVS conditions with HVS mix (3.2% air void content bottom lift, 7.2% air void content top lift and 5% asphalt content), frictionless interface (Case 5)	12,157,000	17,963,000

The permissible ESALs based on subgrade strain are about 2.3 times greater than the simulated HVS ESALs for fatigue cracking for Case 1.

Comparison of the permissible ESALS for Cases 1 and 2 indicates that the HVS conditions were less critical than the design conditions with respect to the subgrade strain criteria. The differences between the HVS and design conditions for this evaluation consisted of the slightly thicker asphalt concrete layer, slightly thinner aggregate subbase layer, and increased base, subbase and subgrade moduli for the HVS conditions. As for Case 1, fatigue is the controlling mode of distress for Case 2, since the permissible ESALs based on subgrade strain are approximately 2.1 times greater than the simulated HVS ESALs to fatigue failure.

The beneficial effect of increased compaction of the asphalt concrete is apparent from comparison of the results for Case 3 and Case 2. Reduction of the air-void content in the standard mix from 8 percent to those obtained in the two lifts of asphalt concrete in Section 502CT pavement increases the permissible ESALs by about 15 percent. This increase results from the larger stiffness of the asphalt concrete resulting from improved compaction.

Comparison of Case 4 with Case 3 shows that substitution of the HVS mix for the standard mix results in a further 10 percent increase in permissible ESALs for subgrade rutting, due to the larger stiffness of the HVS mix. Despite the increase in permissible ESALs, subgrade strain becomes the controlling factor for the allowable repetitions in Cases 3 and 4.

Simulation of a frictionless interface between the two asphalt concrete layers results in a significant reduction in the estimate of permissible ESALs based on subgrade strain, i.e. Case 5 versus Case 4. Permissible ESALs for the frictionless interface condition are about 1/5 of those for the full friction condition.

All of the estimates of permissible ESALs based on subgrade strain are less than the 117,000,000 ESALs applied to the section, which suggests that there may be some conservatism in the Asphalt Institute criteria. The permissible ESALs estimated from the Asphalt Institute criteria should be considered design estimates which will be lower than measured ESALs, although the safety factor is not known at this time.

The results presented in this study support those obtained from Sections 500RF, 501RF, and 503RF that the degree of compaction of the asphalt concrete course and the interface condition between asphalt concrete layers can significantly impact subgrade rutting performance.

4.3 FINDINGS

In general, the analyses reported herein found a correspondence between the Caltrans design estimate of approximately 1,000,000 ESALs and the HVS test measurement of approximately 117,000,000 ESALs. The major impediment to reconciling these two estimates seems to be the inability to accurately quantify effects of the layer interface condition. The following findings of this aspect of the study are considered to have been reasonably well demonstrated and to represent appropriate hypotheses for future inquiry and validation:

1. Fatigue life measurements under full-scale accelerated loading are typically expected to exceed design estimates because design estimates must incorporate a safety factor to minimize the risk of premature failure while accommodating, at the same time, expected variability in testing, in construction, in traffic, and in mix design. For a design reliability level of 90 percent, the computed ratio of simulated HVS ESALs to design ESALs estimated using the fatigue analysis and design system was approximately 3.7.

2. The mixture fatigue analysis and design system proved to be an effective tool for explaining fatigue performance of the HVS pavement. The fact that the actual HVS measurement falls between the estimates for the full friction and frictionless cases for HVS conditions suggests that the analysis and design system may eventually prove useful for structural design as well as for mixture design.

3. According to the Asphalt Institute's subgrade strain criterion, severe subgrade rutting in the HVS pavement would not be expected. Testing of HVS Section 502CT generally confirmed this.

4. The analysis reported herein corroborates prior work showing the importance of good compaction of the asphalt concrete surface to superior fatigue performance. Good compaction of the mix also reduces the contribution of the untreated materials to surface rutting.

5. Loss of bonding at the interface between asphalt-concrete lifts can cause a significant degradation in fatigue life and an increase in subgrade strain leading to increased rutting at the pavement surface.

6. Different mixes, even with similar binders, can result in significantly different fatigue performance. The importance and effectiveness of laboratory fatigue testing and simulation to quantitatively estimate differences in fatigue performance in situ was demonstrated by the analyses presented in this chapter.

CHAPTER 5

SUMMARY AND CONCLUSIONS

5.1 SUMMARY

This report, the fourth in a series detailing the results of the CAL/APT program being performed jointly by UCB and Caltrans, describes the results of the HVS test conducted by the UCB staff on pavement test Section 502CT, an asphalt concrete section containing asphalt treated permeable base. This report also includes: analyses of the performance of the test section; a comparison of its performance relative to the performance of a comparable pavement in the Coastal environment of California; evaluation of the degree of compaction of the asphalt mix on its performance; and, implications of these results relative to current Caltrans pavement construction requirements since the test pavement was constructed according to Caltrans specifications.

HVS trafficking of Section 502CT commenced in December 1995 and was completed in September 1996. A total of 2.67×10^6 load repetitions were applied during this period consisting of 150,000 repetitions of a 40-kN (9,000-lb) half axle load, 50,000 repetitions of an 80-kN (18,000-lb) load, and the remainder with a 100-kN (22,500-lb) load.

The first load associated (fatigue) cracks were observed at approximately 1.3 million repetitions. At 2.67×10^6 load repetitions cracking had reached a level which, according to Caltrans pavement management criteria, resembled a newer pavement that had failed by alligator cracking. The average maximum vertical rut depth at the centerline of the test section at this time was 9.4 mm, less than the Caltrans failure criteria of 12.5 mm. It was noted that

the cracks were hairline (less than 1/32 inch) and pumping was not observed in contrast to typical field sections.

Thicknesses for the pavement sections were selected on the basis of a Traffic Index of 9 (800,000 to 1,200,000 ESALs) and a design "R" value for the subgrade of 10 (measured range—4 to 30) *(2)*. The number of ESALs actually carried according to the Caltrans conversion [(actual axle load/18000)$^{4.2}$] is 117 million, which corresponds to a Traffic Index of 15.9.

When the construction of the test pavements had been completed (April 1995), cores and slabs of the asphalt concrete were taken from the pavement for testing. As with the other three test sections, weakness in the bond (and even a lack thereof) between the two asphalt concrete lifts was observed. At the conclusion of the loading on the test section, a number of cores were taken to check changes in densities of the lifts. When these cores were removed it was noted the two lifts were unbonded and that there was evidence of movement between the lifts resulting from the deflection of the pavement under load. Also, it was observed that the cracking observed at the surface existed only in the top lift; the lower lift was uncracked.

After trafficking densities were measured on cores from the trafficked portion of the pavement, comparisons with the data from the untrafficked section indicated that the air void content of the mix in the top lift was reduced by 2.4 percent (7.6 percent to 5.2 percent) and 1.8 percent in the bottom lift (4.0 percent to 2.2 percent).

5.2 CONCLUSIONS

From the results of tests on Section 502CT and associated analyses, the following conclusions appear warranted.

1. The fatigue analysis and design system developed during the SHRP program and refined within the CAL/APT program has been used to explain the difference between the design estimate for Section 502CT of approximately 1×10^6 ESALs and the HVS measurement of approximately 117×10^6 ESALs. Although some of the discrepancy remains unaccounted for (possibly as a result of difficulties in modeling the bonding between the two lifts of asphalt concrete), the overall agreement helps to validate both the analysis and design system as a mechanism for structural design and the current Caltrans design methodology.

2. As with the other three test sections, results of this HVS test suggest that the Asphalt Institute's subgrade strain criteria for controlling contributions from the unbound reasonable design parameter. Accordingly, these criteria are recommended for use as a part of a mechanistic/empirical analyses to supplement routine Caltrans design procedures in special investigations.

3. Results of the 502CT test support those from Section 500RF and suggest that the Caltrans structural design procedure for a Traffic Index of 9 provides a design reliability of about 90 percent for pavements with asphalt treated permeable base, typical compaction, and representative asphalt concrete mixes. This result is based on the assumption that the stiffness of the ATPB is not reduced by the action of water. Results of a companion study *(4)* indicate that stripping of ATPB may lead to an unconservative design. A companion report *(5)* provides evidence that some Caltrans structural section designs for larger numbers of ESALs may not be sufficiently conservative. The analysis and design system used herein and being refined, in part, through the CAL/APT program, should provide an improved methodology for structural pavement design permitting a higher level of reliability to be obtained for pavements of this type.

4. The recommendations regarding mix compaction and tack coat application resulting from the 500RF, 501RF and 503RF tests are supported by the results from the test on Section 502CT.

REFERENCES

1. California Department of Transportation, *CAL/APT Strategic Plan (July 1995-July 1997)*, adopted by the CAL/APT Steering Committee, May 18, 1995.

2. Harvey, J., L. Du Plessis, F. Long, S. Shatnawi, C. Scheffy, B-W. Tsai, I. Guada, D. Hung, N. Coetzee, M. Riemer, and C. Monismith, *Initial CAL/APT Program: Site Information, Test Pavements Construction, Pavement Materials Characteristics, Initial CAL/HVS Test Results, and Performance Estimates*, Interim Report No. RTA–65W4845–1 for the California Department of Transportation, Institute of Transportation Studies, University of California, Berkeley, April 1996.

3. Harvey, J., L. du Plessis, F. Long, J. Deacon, I. Guada, D. Hung, and C. Scheffy, *CAL/APT Program: Test Results from Accelerated Pavement Test on Pavement Structure Containing Asphalt Treated Permeable Base (ATPB)—Section 500RF*, Report No. RTA–65W4845–3 for the California Department of Transportation, Institute of Transportation Studies, University of California, Berkeley, June 1997.

4. Harvey, J., B. Tsai, F. Long, D. Hung, and C. Monismith, *CAL/APT Program — Asphalt Treated Permeable Base (ATPB), Laboratory Testing, Performance, Predictions, and Evaluation of the Experience of Caltrans and Other Agencies,* Draft Report for the California Department of Transportation, Institute of Transportation Studies, University of California, Berkeley, June 1997.

5. Harvey, J., F. Long, *CAL/APT Program—Comparison of Caltrans and AASHTO Pavement Design Methods*, Draft Report for the California Department of Transportation, Institute of Transportation Studies, University of California, Berkeley, November 1997.

6. Harvey, J., L. du Plessis, F. Long, I. Guada, D. Hung, C. Scheffy, *CAL/APT Program: Test Results from Accelerated Pavement Test on Pavement Structure Containing Untreated Aggregate Base—Section 501RF*, Draft Report for the California Department of Transportation, Institute of Transportation Studies, University of California, Berkeley, September 1997.

7. Harvey, J., D. Hung, J. Prozzi, L. Louw, I. Guada, C. Scheffy, *CAL/APT Program: Test Results from Accelerated Pavement Test on Pavement Structure Containing Aggregate Base—Section 503RF*, Draft Report for the California Department of Transportation, Institute of Transportation Studies, University of California, Berkeley, March 1998.

8. California Department of Transportation, *Highway Design Manual*, Section 600, Sacramento, 1991.

9. Transportek, CSIR, *Guideline to the Use and Operation of the Heavy Vehicle Simulator (HVS)*, March 1995.

10. Sousa, J.B., J. Deacon, S. Weissman, J. Harvey, C. Monismith, R. Leahy, G. Paulsen, and J. Coplantz, *Permanent Deformation Response of Asphalt-Aggregate Mixes*, Strategic Highway Research Program Report No. A-414, National Research Council, Washington, D.C., 1994.

12. Harvey, J., J. Deacon, B. Tsai, and C. Monismith, *Fatigue Performance of Asphalt Concrete Mixes and Its Relationship to Asphalt Concrete Pavement Performance in California,* Report No. RTA-65W485-2 for the California Department of Transportation, Institute of Transportation Studies, University of California, Berkeley, January 1996.

13. Wardle, L.J., *Program CIRCLY, User's Manual, Revision 1*, Geomechanics Computer Program No. 2, Division of Applied Geomechanics, Commonwealth Scientific and Industrial Research Organization, Melbourne, Australia, 1976.

14. Deacon, J., J. Coplantz, A. Tayebali, and C. Monismith, "Temperature Considerations in the Asphalt-Aggregate Mixture Analysis and Design," Transportation Research Record 1454, Transportation Research Board, 1994, pp. 97-112.

15. Harvey, J.T., J.A. Deacon, A.A. Tayebali, R.B. Leahy, and C.L. Monismith, "A Reliability-Based Mix Design and Analysis System for Mitigating Fatigue Distress," *Proceedings*, International Society for Asphalt Pavements, 8th International Conference, Seattle, 10–14 August 1997.

16. Reese, R., Faxed results of comparison of Valley binders aging properties with CAL/APT Goal 1 asphalt-concrete properties. Caltrans Engineering Service Center, Sacramento, October 6, 1995.

17. Santucci, L.E., "Thickness Design Procedure for Asphalt and Emulsified Asphalt Mixes," *Proceedings*, Fourth International Conference on the Structural Design of Asphalt Pavements, University of Michigan, August 1977, pp. 424-456.

11. Shook, J.F., F.N. Finn, M.W. Witczak, and C.L. Monismith, "Thickness Design of Asphalt Pavements—The Asphalt Institute Method," *Proceedings*, Fifth International Conference on the Structural Design of Asphalt Pavements, University of Michigan, August 1982, pp. 17–44.
NOT REFERENCED IN PAPER